PRECONCENTRATION AND SPECIATION OF IRON BY USING RENEWABLE SURFACE FLOW INJECTION SYSTEM (RS-FIA)

A THESIS SUBMITTED TO
THE GRADUATE SCHOOL OF NATURAL AND APPLIED SCIENCES
OF
THE MIDDLE EAST TECHNICAL UNIVERSITY

BY

SERAP TEKİN

IN PARTIAL FULFILLMENT OF THE REQUIREMENTS FOR THE DEGREEOF
MASTER OF SCIENCE
IN
THE DEPARTMENT OF CHEMISTRY

DECEMBER 2003

Approval of the Graduate School of Natural and Applied Sciences.

Prof. Dr. Canan ÖZGEN
Director

I certify that this thesis satisfies all the requirements as a thesis for the degree of Master of Science.

Prof. Dr. Hüseyin İŞCİ
Head of the Department

This is to certify that we have read this thesis and that in our opinion it is fully adequate, in scope and quality, as a thesis for the degree of Master of Science.

Prof. Dr. Mürvet VOLKAN
Supervisor

Examining Committee Members

Prof. Dr. O. Yavuz ATAMAN (Chairman) _____

Prof. Dr. R. Sezer AYGÜN _____

Prof. Dr. Macit ÖZENBAŞ _____

Ass. Prof. Dr. Nusret ERTAŞ _____

Prof. Dr. Mürvet VOLKAN _____

ABSTRACT

PRECONCENTRATION AND SPECIATION OF IRON BY USING RENEWABLE SURFACE FLOW INJECTION ANALYSIS SYSTEM (RS-FIA)

Tekin, Serap

M.Sc., Department of Chemistry

Supervisor: Prof. Dr. Mürvet Volkan

December 2003, 86 pages

The main aim of this study is to combine the sol-gel technology and renewable surface flow injection analysis (RS-FIA) techniques for iron speciation and determination. Thus the home-made FIA system, which consists of 2 syringe pumps and 3 multi-position selection valves, is modified with two flow cells (magnetic cell and jet ring cell) in order to be suitable for renewable surface flow injection technique. All the computer programs used for flow injection analysis are modified to control the whole system automatically. Two different types of solid phase extraction materials are used for the speciation of iron in aqueous systems.

Magnetic beads coated with primary amino groups are utilized for the determination of Fe (III). The magnetic bead reactor is created within the flowing stream by retaining the magnetic beads with a home-made electromagnet. The elution cycle for Fe (III) is done with 0.1 M EDTA solution and determined on-line by transferring to an atomic absorption spectrometer. The spent beads are collected off-line and regenerated.

For the preconcentration of Fe (II), ferrozine doped sol-gel beads are prepared as reactive and disposable surfaces. These beads are handled by the system equipped with a jet ring cell which is connected on-line to a portable UV-VIS fiber optic spectrometer.

Amino sol-gel and ferrozine-doped sol-gel beads are prepared using sol-gel technology and characterized by using surface techniques. Their performances in preconcentration and speciation of iron and the influence of different experimental parameters such as pH, the sequence of reagents, reactor lengths and reaction periods on the flow system are investigated. Renewable surface flow injection analysis is performed by either bead injection or sequential bead injection methods.

Keywords: Renewable Surface Flow Injection Analysis (RS-FIA), Bead Injection Analysis; Sequential Bead Injection Analysis; Iron; Preconcentration; Speciation; Magnetic Beads; Sol-Gel; Jet Ring Cell; Magnetic Cell.

ÖZ

YENİLENEBİLİR YÜZEY AKIŞA ENJEKSİYON ANALİZ SİSTEMİ KULLANARAK DEMİRİN ÖNZENGİNLEŞTİRİLMESİ VE TÜRLENDİRİLMESİ

Tekin, Serap

Yüksek Lisans, Kimya Bölümü

Tez Yöneticisi: Prof. Dr. Mürvet Volkan

December 2003, 86 sayfa

Bu çalışmanın temel amacı sol-gel teknolojisi ile yenilenebilir yüzey akışa enjeksiyon analiz tekniklerini birleştirerek demir iyonlarının ön zenginleştirilmesi ve türlendirilmesini sağlamaktır. İki adet şırınga pompası ve üç adet çok yönlü seçmeli vanadan oluşan ve bölümümüzde geliştirmiş olduğumuz akışa enjeksiyon sistemi iki akış hücresi (manyetik hücre ve jet halka hücre) ile desteklenerek yenilenebilir yüzey akışa enjeksiyon tekniğine uygun hale getirilmiştir. Akışa enjeksiyon analizi için kullanılan bütün bilgisayar programları, tüm sistemi otomatik olarak kontrol edecek şekilde değiştirilmiştir. Sulu sistemlerdeki demiri türlendirebilmek için, iki farklı türde katı faz çıkarma maddesi kullanılmıştır.

Fe (III) tayini için, birincil amino grupları kaplanmış manyetik parçacıklar kullanılmıştır. Manyetik parçacık reaktörü, akış halindeki parçacıkların ev-yapımı bir elektromıknatıs içinde tutulmasıyla oluşturulmuştur. Fe (III) geri kazanım döngüsü 0.1 M EDTA çözeltisiyle yapılmış ve atomik absorbsiyon spektrometresine gönderilerek tayin edilmiştir. Kullanılmış parçacıklar akış sistemi dışında toplanmış ve tekrar kullanılabilir hale getirilmiştir.

Fe (II) önzenginleştirmesi için reaktif ve atılabilir yüzey olarak ferrozin içeren sol-jel tanecikleri hazırlanmıştır. Bu tanecikler, jet halka hücre ile donatılmış ve portatif bir UV-VIS fiber optik spektrometreye bağlı olan sistemde kontrol altında tutulmuştur.

Amino sol-jel ve ferrozin içeren sol-jel tanecikleri, sol-jel teknolojisi kullanılarak hazırlanmış ve yüzey teknikleri kullanılarak karakterize edilmiştir. Hazırlanan reçinelerin demir iyonlarını önzenginleştirme ve türlendirmedeki performansları ile pH, reaktör uzunlukları ve reaksiyon süreleri gibi çeşitli deneysel parametrelerin akış sistemi üzerindeki etkileri incelenmiştir. Yenilenebilir yüzey akışa enjeksiyon analizi, tanecikli enjeksiyon ya da ardışık tanecikli akışa enjeksiyon yöntemleriyle yapılmıştır.

Anahtar Sözcükler: Yenilenebilir Yüzey Akışa Enjeksiyon Analizi; Tanecikli Akışa Enjeksiyon Analizi ; Ardışık Tanecikli Akışa Enjeksiyon Analizi ; Demir ; Önzenginleştirme; Türlendirme; Manyetik Tanecikler; Sol-jel; Jet Halka Hücre; Manyetik Hücre.

To the Dear Memories of
My Father and My Grandmother

ACKNOWLEDGMENTS

I would like to express my gratitude to Prof. Dr. Mürvet Volkan for her encouragement, guidance and care. She was always with me whenever I needed help. I feel so lucky that she was my supervisor.

I am also very grateful to Prof. Dr. Macit Özenbaş and Prof. Dr. O. Yavuz Ataman for their support and guidance throughout this study.

Special thanks go to David A. Holman and Garth Klein for their assistance and contribution in building up this thesis.

Special thanks are extended to Necati Koç, Sevim Ulupınar and Serpil Selvi for their kind helps. I would also like to thank all the analytical chemistry group members.

Very special thanks go to my dear friend Murat Kaya for his sincere help at any time.

Finally, my sincere thanks go to my mother, sister and Cemo for their patience and support throughout my life.

TABLE OF CONTENTS

LIST OF TABLES

TABLE

LIST OF FIGURES

FIGURE

CHAPTER 1

INTRODUCTION

1.1 The Sol-Gel Technology

Although noticed as early as 1846 and known to play a part in natural processes like the formation of the end products such as opal, it is mainly during the post-World War II period that the Solution-Sol-Gel (S-S-G) commonly known as the Sol-Gel (S-G) process has been increasingly exploited for the preparation of glasses and other ceramic materials [1].

Sol-gel processing methods were first used historically for decorative and constructional materials. In the last century, many new applications were developed on a more scientific basis as new characterization techniques became available. Today, sol-gel methods are reaching their full potential, enabling the preparation of new generations of advanced materials not easily accessible by other methods yet using mild, low-energy conditions [2].

Sol-gel has many application areas such as

- Optics (coating, filters, solar cells, magneto optics)
- Protective coatings on metals and polymers
- Ferroelectrics, semiconductors, dielectrics, sensors
- Encapsulation of molecules, enzymes, cells, solid electrolytes, binders and actuators [3].

1.1.1 The Sol-Gel Process

Sol-gel materials encompass a wide range of inorganic and organic/ inorganic composite materials which share a common preparation strategy. They are prepared via sol-gel processing involving the generation of colloidal suspensions "sols" which are subsequently converted to viscous gels and hence to solid materials [4]. The main stages of sol-gel processing are described below:

Hydrolysis

The first step occurs by the hydrolysis of a silicon alkoxide ($Si(OR)_4$) with water.

$$Si(OR)_4 + nH_2O \rightarrow Si(OR)_{4-n}(OH)_n + nROH$$

During the hydrolysis reaction, alkoxide groups are replaced with hydroxyl groups.

Condensation

Condensation reactions can be either water or alcohol condensation.

≡Si─OH +HO─Si≡ → ≡Si─O─Si≡ + H_2O (water condensation)

≡Si─OR +HO─Si≡ → ≡Si─O─Si≡ + ROH (alcohol condensation)

Condensation reactions involving the silanol groups produce siloxane bond (Si─O─Si).

Gelation

Gelation occurs when links form between silica sol particles, produced by hydrolysis and condensation. A spanning cluster is formed, giving a network which entraps the remaining solution, with high viscosity.

Ageing

A range of processes, including formation of further cross-links, associated shrinkage of the gel as covalent links replace non-bonded contacts.

Drying

The loss of water, alcohol and other volatile components, first as syneresis (expulsion of the liquid as the gel shrinks), then as evaporation of liquid from within the pore structure with associated development of capillary stress which frequently leads to cracking. This may also include supercritical drying, in which capillary stress is

avoided by the use of supercritical fluids (e.g. CO_2) in conditions where there are no liquid/vapour interfaces [2].

Densification

Thermal treatment leading to the collapse of the open structure and formation of a dense ceramic. Heating the porous gel at high temperatures causes densification to occur [4].

There are three approaches used to make sol-gel monoliths:

- Gelation of a solution of colloidal powders
- Hydrolysis and polycondensation of alkoxide precursors followed by hypercritical drying of gels
- Hydrolysis and polycondensation of alkoxide precursors followed by aging and drying under ambient atmospheres [5].

Sol-gel has many advantages over commonly used organic polymers;

- inherent flexibility associated with material preparation and processing
- control of microstructure (pore size distribution, specific surface area)
- highly porous and nanocrystalline materials can be synthesized
- the use of liquid precursors allow the production of thin films, fibers and monoliths
- materials which contain both inorganic and organic polymer networks can be produced
- reagents can be readly incorporated in a stable host matrix by simply adding them to the sol prior to its gelation.

- covalent attachment of organic and biological species to porous silicate glass structures possible
- high homogeneity, optically transparency, chemical and mechanical stability and purity of the resulting materials
- mild chemical conditions and lower processing temperature [6].

1.1.2 Organically Modified Silicate Materials (ORMOSILs)

Sol gel process provides a convenient method for the production of organically modified surfaces by incorporating alkoxysilane monomers that contain desirable functional groups in the starting polymerization mixture [2, 7].

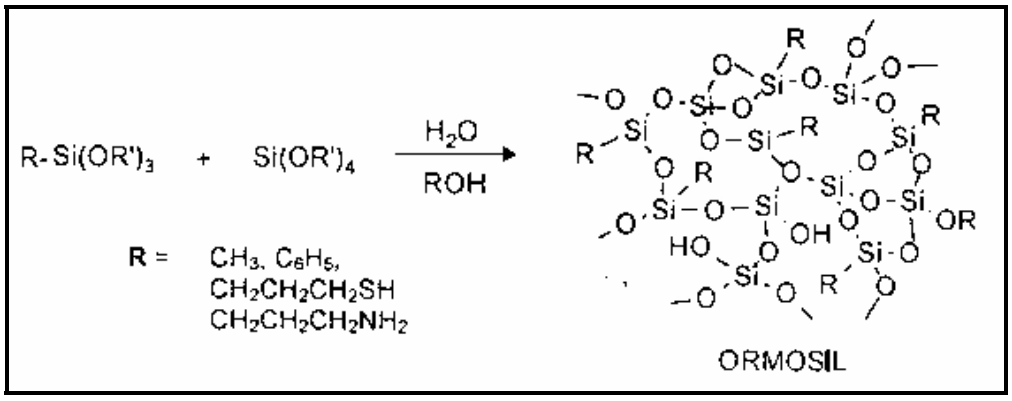

Figure 1.1 ORMOSIL

The blending of inorganic precursors (e.g. tetramethoxysilane; TMOS) with organoalkoxysilanes can lead to materials with properties better than those prepared alone. These materials termed organically modified silicates (ORMOSILs) (Figure 1.1), can be

prepared by mixing organosilicon precursors of the general formula $(R_{4-x}Si(OR')_x$, where R represents the desirable reagent or functional group and x is 1-3, with TMOS, or alternatively alone. Specific functional groups that have been used include CH_3, C_2H_5, C_6H_5, $(CH_2)_3NH_2$, $(CH_2)_3SH$ [7, 8].

Relative to the pure inorganic glasses, ORMOSILs possess many advantages including:

- Flexibility of the silica gel can be improved thus enabling thick, crack-free films to be prepared and utilized
- Specific functional groups can be covalently attached to the silicon-oxygen network
- Reactive functional groups can be introduced in the matrix which can be subsequently used to anchor molecular recognition groups on the matrix
- Relative to physically entrapped species, higher concentrations of reagents can be incorporated into the matrix [8].

ORMOSILs have promising future in analytical science. They can be used to change the porosity, hydrophobicity, and flexibility of silicate sol-gel derived glasses. They can also be used to chemically attach a suitable reagent to the inorganic framework [8, 9].

Several organically modified materials were prepared by using polyethyleneglycol (PEG) [10], 3-aminopropyltriethoxysilane (APTES) [11], γ-aminopropylsilanetriol (APSTOL) [12], 3-glycidoxy

propyltrimethoxysilane (GPTMS) [13] and poly (dimethylsiloxane) (PDMS) [14] as organoalkoxysilanes.

Various reagents such as proteins [15], enzymes [16], antibodies [17], particles, metals such as Fe (III) [18], Ni (II) and Co (II) [19], Cr (III) [20], Cu (II) [21], and Eu (III) [22], organics such as aromatic oxygen palladiumphthalocyanine [23], zinc tetrasulfophthalocyanine [24], aluminum tetrasulfophthalocyanine chloride [25], chelating agents [26], indicator dyes [27, 28], zeolites, cyclodextrins and crown ethers [29] were physically entrapped in the sol-gel structures.

For iron determination, pyoverdin, a natural fluorescent pigment biosynthesized by Pseudomonas fluorescence, was entrapped in sol-gel glass [30] and capillary glass tubes filled with porous sol-gel silica powder were doped with o-phenanthroline [31]. Ferrozine, an iron indicator, was immobilized in a sol-gel derived PDMDAAC-SiO_2 (where PDMDAAC stands for poly(dimethyldiallylammonium chloride), composite thin films via ion-exchange were prepared [32].

Magnetic nanoparticles can be prepared by the sol-gel process by doping γ-Fe_2O_3 (maghemite) [33-37], Fe_3O_4 (magnetite) [38,39], α-Fe_2O_3 (hematite) [40], ferromagnetic metallic Ni [41,42] and by coprecipitation of Fe^{2+} and Fe^{3+} [43]. Magnetic particles (microspheres, nanospheres and ferrofluids) are widely studied for their applications in various fields in biology and medicine such as enzyme and protein immobilization, genes,

radiopharmaceuticals, magnetic resonance imaging MRI, diagnostics, immunoassays, RNA and DNA purification and magnetically controlled transport of anti-cancer drugs [43].

1.2 Preconcentration and Speciation of Iron

Iron is one of the most important elements in environmental and biological systems. The environmental and biological effectiveness of iron depends on its chemical properties, such as valence, solubility, and the degree of chelation or complex formation. Determination of total iron content in these systems is not a sufficient criteria for estimating its ecological effect. Iron is a significant factor in the evaluation of water quality, and its reactivity also drives numerous chemical processes in natural waters [44-46].

Most methods for the determination of Fe (III) are based on colorimetric determination of the Fe (II) concentration, followed by a separate determination of the total Fe concentration after reduction of Fe (III). The difference between the concentration of total iron and that of Fe (II) is taken as the Fe (III) concentration. These methods lack sufficient sensitivity for determining iron in water samples at ppb or sub ppb levels. As a result, preconcentration and separation techniques are usually required before analysis [44].

A critical requirement for the analysis of iron in many environmental samples is the discrimination between Fe (II) and Fe (III). Atomic spectrometry is both sensitive and selective, but does not meet this

criteria. Flow injection analysis, has the potential to overcome these problems [47].

1.3 Flow Injection Analysis

Although conceived in Denmark, it was in Brazil during the late 70's at the Centro de Energia Nuclear na Agricultura (CENA) where flow injection analysis (FIA) was demonstrated, for the first time, to be a practical and useful analytical tool. Indeed, by 1978 50% of all the papers published world-wide originated at CENA (where at that time 40000 samples were analyzed yearly by FIA). Since then, the scope of applications has grown world-wide, and flow injection analysis has become a major analytical technique described in over 8000 papers [48-54].

Flow injection (FI), the first generation of FIA techniques, is the one most widely used. In its simplest form, the sample zone is injected into a flowing carrier stream of reagent. As the injected zone moves downstream, the sample solution disperses into the reagent, while a product begins to form at interfaces between the sample zone and the reagent. A detector placed downstream records a desired physical parameter as it changes due to the passage of the sample material through the flow cell [48, 54] (Figure 1.2).

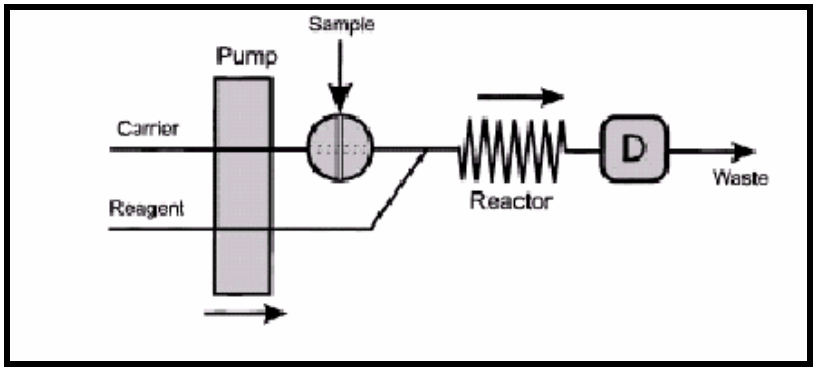

Figure 1.2 Flow Injection System

Flow injection analysis offered opportunities to perform unique assays that are not feasible when performed manually. This finding led to the definition of FI as a means of information–gathering from a concentration gradient formed from an injected, well-defined zone of a fluid, dispersed into a continuous unsegmented stream carrier [48].

Automated sample processing, high repeatability, adaptability to microminiaturization, containment of chemicals, waste reduction, and reagent economy in a system that operates at μL levels are all valuable assets that contribute to the application of FI to real-world assays. Yet, the main assest of FI are the well-defined concentration gradient that forms when an analyte is injected into the reagent stream and the exact timing of fluidic manipulation [48, 52, 55].

The transition from continuous to discontinuous reversed-flow mode was facilitated by the proliferation of personal computers and availability of automated high precision syringe pumps and valves. Thus, FIA changed from FI to sequential injection (SI) and most recently to bead injection (BI) [55].

As FI developed, it assimilated and grew with technological advances-automated valve-based injectors, stepper-motor-driven high-precision syringe pumps, and scanning flow through detectors [55].

1.3.1 Sequential Injection

The sequential injection (SI) technique was developed to satisfy the demands for mechanically simple and robust, yet versatile, flow injection (FI) methodology [56, 61].

Sequential injection, the second generation of FIA techniques, is the most versatile one. Sequential injection, where sample and reagent zones are stacked in a tubular conduit, merged by means of flow reversal of the carrier stream and then transported into the detector. In its simplest form, the sample zone is injected along with a zone of reagent into a carrier stream. During flow reversals of the carrier stream, the sample and reagent zones disperse within each other, while on their interface the reaction product is formed. A flow through detector records changes in a desired physical parameter when the reaction product reaches the flow cell. The underlying principle of sequential injection is the flow programming [57, 62, 63].

Sequential injection uses programmable, bi-directional discontinuous flow, precisely choreographed by means of computer control. Sample and reagents are injected sequentially, by means of a multi-position valve, into a carrier stream using a single syringe pump placed upstream of the valve [64].

Besides its versatility and mechanical simplicity, the SI technique offers additional advantages, namely the ability to change experimental parameters without physical restructuring of the manifold and the ability to control reaction time and the degree of zone dispersion [60, 61].

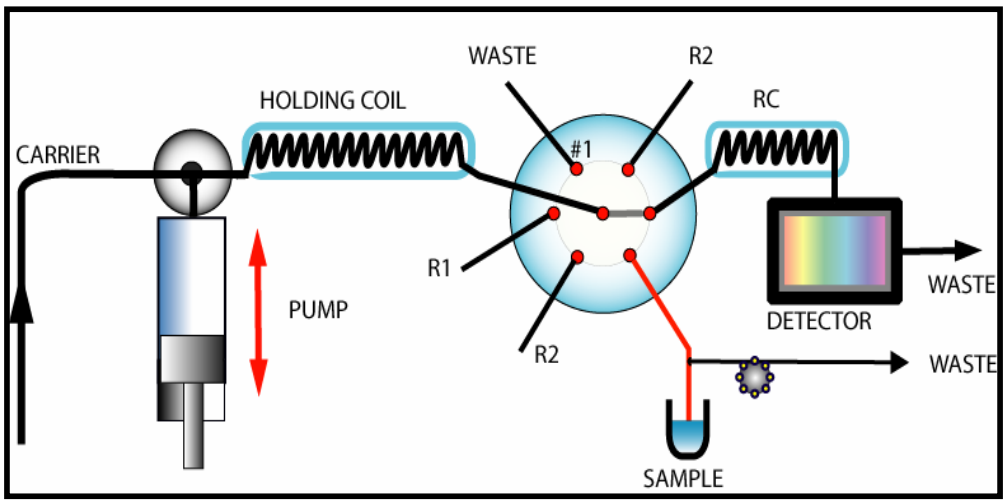

Figure 1.3 A Conventional Sequential Injection Setup [64].

A conventional SI setup (Figure 1.3) comprises a bi-directional syringe pump, holding coil, multi-position valve, reactor coil (RC) and detector [56]. A high resolution stepper motor driven pump is, along with the multi-position valve, controlled by computer and dedicated software. In a typical assay cycle, sample and reagent are sequentially aspirated into the holding coil, forming a stack of well defined zones, which is transported into the detector by a flow reversal. Flow programming and random access to sample and reagent solutions, provided by a multi-position valve, yield unprecedented versatility since all parameters – sample injection, solute dispersion and timing

are controlled by software adjustments without the need for physical reconfiguration of the system. Therefore, open architecture software is a key component of sequential injection system [64].

Both flow injection (FI) and sequential injection (SI) analysis can be carried out in the bead injection (BI) format. Indeed, SI is the perfect vehicle for BI which in turn enhances SI by eliminating the problem of mixing reactants during the loading process [60, 65].

1.3.2 Bead Injection

Bead injection, the third generation FIA technique, is the most advanced to date. In its simplest form, microspheres are injected into a conduit, where they are trapped at a selected location. Next, the sample zone is injected and perfused through the beads, while sample components react with functional groups on bead surfaces. Retained analyte molecules are detected by spectroscopy in their native form, or reacted in situ with suitable color or fluorescent reagents. Analyte molecules may also be eluted for detection downstream. At the end of the assay protocol the beads are, by means of flow reversals, transported into a different location or discarded to waste (Figure 1.4). The unique features of bead injection are high precision of bead delivery, absence of carryover and fast automated renewal of the reactive solid phase that is delivered in uniform composition throughout the series of measurements [64].

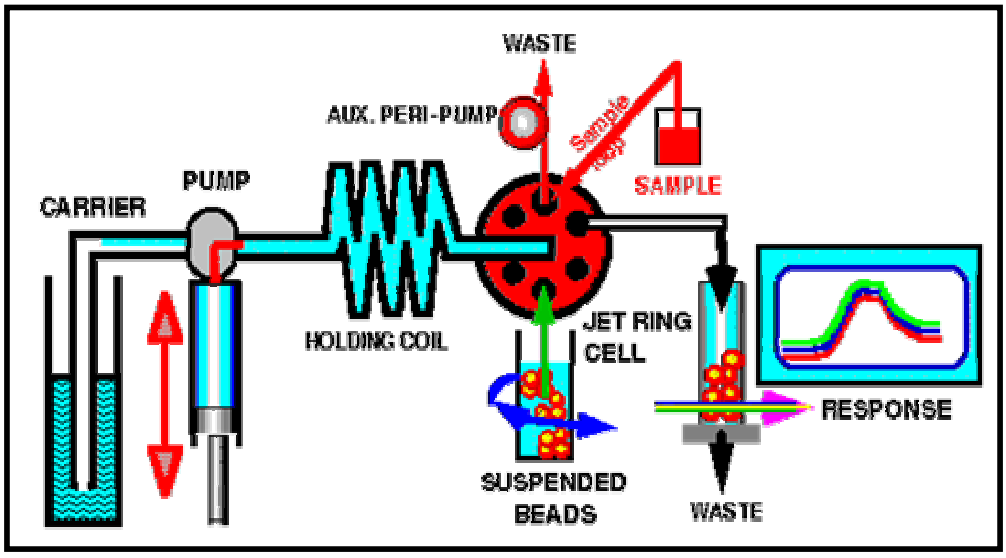

Figure 1.4 A Conventional Bead Injection Setup [64].

Bead injection combines the advantages of solid-phase chemistry with the novelty of fluidic handling of microcarrier beads, allowing automated surface renewal and postanalysis manipulations. Surface renewal is an especially critical feature because assay surfaces become contaminated or otherwise dysfunctional with repeated use. Bead injection does not have these constraints [60].

The BI system uses an open architecture in which the hardware remains the same while the chemistries and computer control are changeable; the same basic instrument can be easily configured to perform a variety of assay in a dedicated or a sequenced fashion [56, 60].

1.3.3 Renewable Surface-Flow Injection Analysis

The use of renewable surface techniques in flow injection systems initiated a new approach in solid-phase separations and detection by providing a scaleable fluidics system to reproducibly deliver selective microparticles to a separation or sensing flow cell [60].

The technique is based on the handling of microparticle suspensions and the temporary and periodic immobilization of these solids as close as possible to the detector system. This technique combines the advantages of solid-phase chemistry with the novelty of the fluidic handling of microcarrier beads, allowing automated surface renewal and different analytical procedures [58, 60].

By releasing the used particles and delivering fresh particles for each new sample, the interactive surfaces are renewed for each separation or sensing measurement (hence the term "renewable surfaces"). The manipulation of microspheres, or "beads", in a SI fluidic system has been described as "bead injection" while the use of captured particles for separations has been referred to as "renewable surface flow injection analysis" (RS-FIA) [58].

FI renewable surface methods have now been used in a variety of chemical and biological applications with flow cell mechanisms including moveable capillaries, moveable barriers with leaky tolerances, porous frits, and magnetic capture cells containing magnetic flux conductors. FI or SI assays, with or without renewable

surface techniques, have focused primarily on single analyte or single particle type analyses in a serial fashion [66].

RS-FIA systems offer the following advantages:

- The reactive surface needs not to be regenerated, saving time, reagents and solvents
- No hysteresis, nor carryover will any longer be caused by the imperfect regeneration of sensor surfaces, membranes or stationary phase
- Reactive groups will no longer need to be permanently attached to the reactive or sensing surfaces
- Often physical adsorption of the reagents will suffice
- The instrument or chemical sensor system based on RS-FIA will be versatile, since different kinds of reactive beads can be selected and automatically introduced into monitored area at will
- The analyte will become preconcentrated from a larger sample volume onto a small surface within sight of a detector
- The chemical reactions and adsorption/desorption mechanism will not need to be reversible since the reacted surface will be disposed off [66, 67].

The beads used range from non-conducting (glass), conducting (graphite particles), to magnetic materials. Beads or microparticles are available with a wide variety of surface functional groups, material

properties, and sizes and have the possibility of reaction kinetics similar to those found in free solution [65].

The key component of the RS-FIA system is the flow cell. The jet ring cell, a specialized detector flow cell, is the first renewable microcolumn which was developed by Ruzicka and co-workers [66-68].

The jet ring (JR) cell must provide the following functions: trap and release beads, direct liquid flow uniformly throughout the packed beads, allow monitoring of bead layers by fiber optics and maintain and reproduce the geometry of the bead column throughout a series of experiments [69, 70].

The working principle of the jet ring cell can be summarized in a five step protocol:
Beads are introduced (1), captured (2), perfused by analyte (3), perfused by carrier solution (4), and discharged (5) when the measurement is completed [59]. These steps are shown in Figure 1.5.

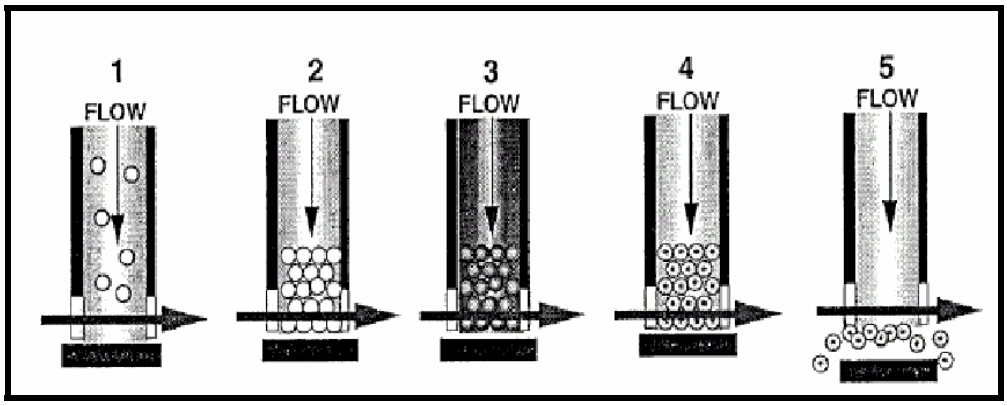

Figure 1.5 Working Principle of Jet Ring Cell.

The use of monosized magnetic beads offers the convenience of magnetic separation. These particles are superparamagnetic, meaning that they respond to a magnetic field, but demagnetize completely when the field is removed. Thus, the microparticles can be separated easily from the liquid phase with an external magnet, but can be redispersed immediately after the magnet is removed [65, 66].

The magnetic bead reactor is created within the flowing stream with an electromagnet to form an open tube reactor. Renewable reaction surface is formed with magnetic beads. The typical experimental protocol is as follows:

1. The magnetic beads coated with specific functional groups are aspirated into the reaction coil which is located within an electromagnetic field.

2. Turning on the electromagnet traps the beads within the coil to form an immobilized reaction surface.

3. The sample solution is aspirated into the reaction coil and the flow is stopped for a specific contact time. This contact time can vary to cover a dynamic range from initial binding to equilibrium.

4. The sample mixture is discharged to the detector by an elution step and this yields a signal at the detector which can be related to the analyte concentration.

5. The electromagnetic field is turned off and the reactor contents are flushed to waste [71, 72].

1.3.4 Determination of Iron by Flow Injection Analysis

Conventional batchwise procedures are usually time-consuming and labor-intensive, require large sample volumes, and are prone to contamination and analyte loss. Therefore, interest has been growing in flow injection on-line separation and preconcentration for atomic spectrometry and element mass spectrometry not only for sample introduction but also for sample pretreatment such as analyte preconcentration and separation from the bulk of the matrix [56, 62].

Flow injection techniques have attracted extensive interest for the trace analysis of iron that these systems are in many cases portable, analyses are rapid, sample handling is minimal, only small volumes are required and the precision and limits of detection are good [73-75].

The extraction of metals as their chelates from aqueous samples can be simplified, miniaturized and automated by flow injection/sorbent extraction techniques. In-line preconcentration and matrix removal in flow-injection analysis for flame or plasma spectrometry is a well established technique, allowing up to 100-fold increases of sensitivity and of the limit of detection [76].

Several iron speciation procedures suitable for FIA applications have been proposed. Thus, a flow injection device coupled to that becomes an ideal system for rapid on-line preconcentration and speciation for metals.

Several approaches have been followed for the simultaneous determination of iron (II) and iron (III) by flow-injection method. The flow injection system was mainly coupled with spectrophotometer [77-85], luminol chemiluminescence detection [86-88], ICP-MS [89], ET-AAS [90], FAAS [91-97], UV-VIS [94] and ICP-AES [98].

For the preconcentration of iron, C_{18} phase column which is impregnated with ferrozine [78], melamine-formaldehyde resin [79], microporous Amberlite XAD-4 functionalized by N-hydroxy ethylenediamine (HEED) groups [86], 8-hydroxyquinoline chelating resin [88], macrocycle immobilized silica gel [91], chelating resin Chelex-100 [93, 95], 2-Mercaptobenzimidazole loaded on silica gel (MBI-SG) [94], C_{18} bonded silica material [89, 96], 8-hydroxy quinoline immobilized on vinyl polymer gel [99] and ion-exchange dual columns were used. Redox systems were also used for the determination of iron [100].

1.4 The Aim of This Work

A renewable surface flow injection analysis (RS-FIA) system was designed for on-line preconcentration and speciation of trace level concentrations of iron.

The home-made flow injection system was modified with two flow cells; a jet ring cell and a home-made magnetic cell. The computer programs used for the flow injection system were modified to control

the whole system automatically. The system was coupled with a UV-VIS and atomic absorption spectrometer simultaneously.

A magnetic cell was designed for the determination of Fe (III). Commercially available superparamagnetic beads coated with primary amino groups were utilized for the speciation of Fe (III). This was a novel type of bead injection for trace analysis since magnetic separation and magnetic beads have not been applied to the FIA system for the preconcentration and speciation of inorganic ions.

The jet ring cell was used for the determination of Fe (II). Sol-gel technology was used for the preparation of the resins used as renewable sensing surfaces for bead injection. A novel type of sol-gel namely “ferrozine-doped sol-gel” was prepared for the speciation of Fe (II). It was aimed to determine Fe (II) and Fe (III) separately without any further oxidation/reduction step.

CHAPTER 2

EXPERIMENTAL

2.1 Chemicals and Reagents

i) **Fe (III) stock solution (1000 mg L^{-1}):** Prepared by dissolving 0.484 g ferric chloride hexahydrate; $FeCl_3.6H_2O$ (Fisher), in 100 mL de-ionized water. Working standard solutions were prepared from the stock solution by appropriate dilution using 0.1 M acetate (pH 4.5) buffer solution, 1 M HCl or 0.1 M EDTA.

ii) **Fe (II) stock solution (500 mg L^{-1}):** Prepared by dissolving 0.249 g ferrous sulfate heptahydrate; $FeSO_4.7H_2O$ (Analar), in 100 mL 1.3 mM hydroxylamine hydrochloride (Carlo Erba) to prevent oxidation of iron (II). Working standard solutions were prepared from the stock solution by appropriate dilution using 0.14 M HMTA (pH 5.5) buffer solution.

iii) Fe (III) AAS stock solution (1000 mg L^{-1}); Aldrich.

iv) Dynabeads M-270 Amine, Dynal Biotech.

v) γ-Aminopropyl trimethoxy silane, Aldrich.

vi) Tetraethoxysilane (TEOS), 98%, Aldrich.

vii) Tetramethoxysilane (TMOS), Aldrich.

viii) Hydrochloric acid, 35%, extra pure, Merck.

ix) Acetic Acid, glacial, 100 %, extra pure, Merck.

x) Sodium acetate, Fisher.

xi) Ethanol, HPLC grade, Aldrich.

xii) Methanol, extra pure, Merck.

xiii) Ethylenediaminetetraacetic acid (EDTA) solution (0.1 M): Prepared by dissolving 2.92 g EDTA (Surechem Products Ltd.) in 100 mL de-ionized water.

xiv) Ferrozine solution (1000 mg L^{-1}): Prepared by dissolving 0.1 g ferrozine; (3-(2-pyridyl)-5,6-diphenyl-1, 2, 4-triazine-p, p'-disulfonic acid, monosodium salt hydrate) (Aldrich), in 100 mL de-ionized water.

xv) Polydimethyldiallylammonium chloride (PDMDAAC), 20% (weight in water), Aldrich.

xvi) Hexamethylene-tetramine (HMTA), Fisher.

All other reagents were of analytical reagent grade. De-ionized water obtained from a Millipore water purification system was used for sample and standard preparations. All the glass and plasticwares were soaked in 10% HNO_3 for at least 24 hours and then rinsed with de-ionized water (18 MΩ cm^{-1}).

2.2 Apparatus

All spectrophotometric analysis for Fe (III) determination were performed with a Philips PU 9200 atomic absorption spectrometer.

A Thermo Elemental iron hollow cathode lamp was used as radiation source. The instrumental parameters used are given in Table 2.1.

Table 2.1 Instrumental Parameters Used for the Determination of Fe (III)

Light Source	Iron Hollow Cathode Lamp
Wavelength	248.3 nm
Band Pass	0.2 nm
Lamp Current	15 mA
Flame for Atomization	Air-Acetylene
Burner Slot	50 mm

Fe (II) determination studies by the RS-FIA system were performed with an AvaSpec-2048 UV-VIS Fiber Optic (SMA terminated) portable spectrometer using the analytical wavelength range of 561-563 nm. The software package AvaSoft 5.1 Full Version was used to control the spectrometer. For the batch type studies, a Shimadzu UV-VIS 160 spectrometer was used.

2.2.1 The Home-Made Flow Injection System

The home-made flow injection system (Figure 2.1) consisted of 2 Kloehn model 50300 (24k increments, 6 cm stroke) bi-directional syringe pumps controlled by command logic via RS485 and 3 Kloehn model 50120 Intellect valves (5-way distribution) (Figure 2.2). Kloehn syringes from 500 µL to 50 mL were available.

The system was computer-controlled and the software package Kloehn Beta Version 0.8 was used to control the whole system.

The FIA system designed, was arranged for the determination of both oxidation states of iron; iron (II) and iron (III). The system was modified with a magnetic cell and a jet ring cell. The use of bi-directional syringe pumps and the flow cells allowed the application of both sequential and bead injection analysis methods on the system. All the connections were done by Kloehn PTFE tubings of outer diameter (od) 1/16´´- 1/8´´ and inner diameter (id) 1/16´´- 1/32´´.

Figure 2.1 The Home-Made Flow Injection System

Figure 2.2 50300 syringe drive module (**1**) and 50120 intellect valve driver (**2**)

2.2.2 Magnetic Cell

A home-made magnetic cell was used for Fe (III) determination in which commercially available superparamagnetic beads (Dynabeads M-270 Amine) were used. Two types of electromagnet designs were investigated and examined. The first electromagnet was made by wrapping a 15 x 50 x 15 mm^3 block of soft steel with fine magnetic wire (od 0.40 mm). The flow path was placed in the magnet by cutting a 5-mm channel on the steel block. The dimensions of the faces were 5 x 50 mm^2 (Figure 2.3).

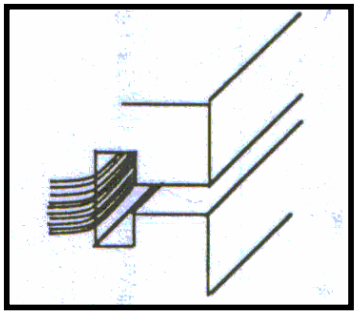

Figure 2.3 Electromagnet Design 1

The second electromagnet was made by modifying a transformer to create a field. A 5-mm channel was cut in one of the arms of the transformer (Figure 2.4). The dimensions of the face were 10 x 35 mm. Both electromagnets were supplied with a constant dc voltage of 5 V and 1.5 A.The beads used in the magnetic cell were kept in suspension by using a vortex mixer (REAX top, Heidolph).

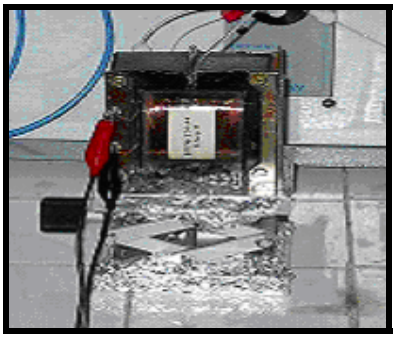

Figure 2.4 Electromagnet Design 2

2.2.3 Jet Ring Cell

The system was modified with a FIAlab Jet Ring Cell (Figure 2.5); a renewable bead column system including a valve actuated flow cell and fiber optic (400 μ) connections, in order to perform bead injection for the determination of Fe (II). The fiber optic connections to the spectrometer were SMA-terminated and a steel sheet was coated around the fibers that slide into the jet ring cell.

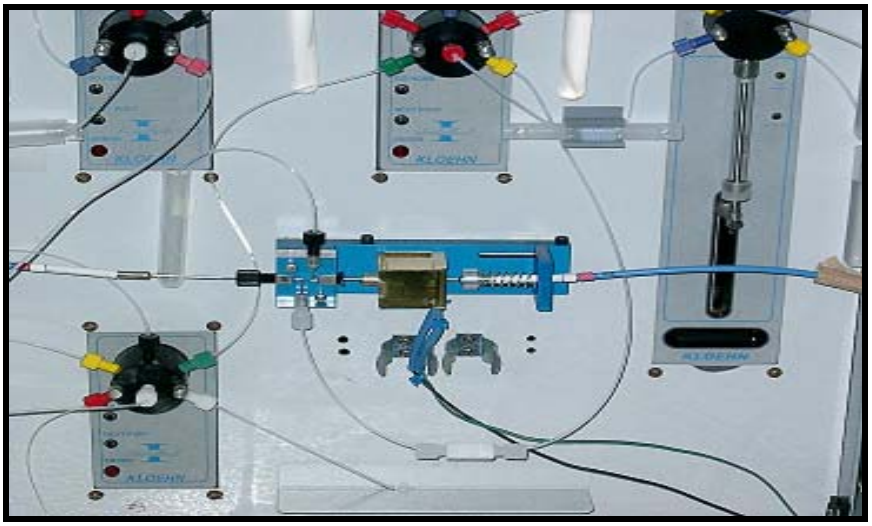

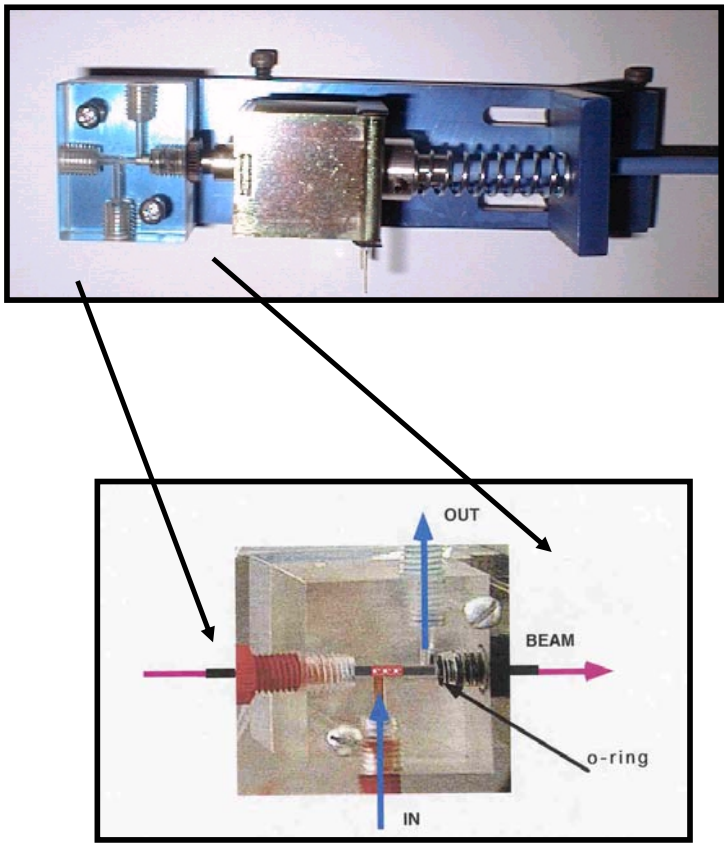

Figure 2.5 Jet Ring Cell

Jet ring cell is a specialized flow cell that traps the beads in a geometry that allows uniform perfusion. It consists of a flat surface

valve positioned perpendicular to flow tube, leaving a narrow circular gap. The configuration of the jet ring cell for absorbance measurement allows the use of transparent beads as solid surface and monitoring by fiber-optic-based spectrophotometry. The beads used in the jet ring cell were kept in suspension by using a rotating table (Alitea Instruments). A 24 dc V supply was used to activate the cell. In order to open the cell and release the beads, voltage was applied and to close the cell and trap the beads the voltage was removed.

2.3 Preparation of the Sol-Gel Resins

2.3.1 Preparation of the Sol-Gel Beads

Type 1: 5 mL TEOS, 5.4 mL ethanol and 1.6 mL de-ionized water were mixed immediately. After adjusting the pH to 4.5 with 2.10^{-4} M HCl, the mixture was stirred with a magnetic stirrer for 30 minutes.

Type 2: 4 mL TEOS, 8 mL de-ionized water, 0.6 mL 4 M HCl and 0.4 mL ethylene glycol were mixed and the mixture was stirred for 30 minutes.

Type 3: 1 mL TMOS, 0.250 mL de-ionized water and 0.0140 mL 0.050 M HCl were mixed and the mixture was stirred for 15 minutes in an ultrasonic shaker.

Type 4: 2.5 mL TMOS, 0.5 mL de-ionized water and 0.5 mL 0.0010 M NaOH were mixed and the mixture was stirred for 30 minutes.

Then, all sols were allowed to gel at room temperature for 3 days in closed containers and dried to constant weight at 60 °C for approximately one week. After drying, the sol-gel monoliths obtained were crushed in a porcelain cup and sieved. The fractions of various particle sizes were collected for further experiments.

2.3.2 Preparation of Amino Sol-Gel Resin

Type 1: 5 mL TEOS, 5.4 mL ethanol and 1.6 mL de-ionized water were mixed and the pH was adjusted to 4.5 with 2.10^{-4} M HCl. 550 μL γ-aminopropyltrimethoxy silane was added to the above mixture dropwise. The mixture was stirred for 30 minutes.

Type 2: 1 mL TEOS, 1 mL ethanol and 0.32 mL pH 4.5 acetate buffer were mixed and the mixture was stirred for 30 minutes. 110 μL amino silane was diluted to 1 mL with ethanol and added to the above solution dropwise. The mixture was stirred for 1 hour.

Type 3: 1 mL TEOS, 1 mL ethanol and 0.35 mL 1 M HCl were mixed and the mixture was stirred for 30 minutes. 110 μL amino silane was diluted to 1 mL with de-ionized water and added to the above solution dropwise. The mixture was stirred for 1 hour.

Type 4: 1 mL TEOS, 1 mL ethanol and 1 mL 1 M HCl were mixed immediately and the mixture was stirred for 30 minutes. 100 μL amino silane was diluted to 1 mL with ethanol and added to the above solution dropwise. The mixture was stirred for 1 hour.

Type 5: 5 mL TEOS, 5.4 mL ethanol and 1.6 mL 1 M HCl were mixed immediately and the mixture was stirred for 30 minutes. 500 μL amino silane was diluted to 5 mL by 1 M HCl and added to the above solution dropwise. The mixture was stirred for 1 hour.

Then, all sols (Type 1-5) were treated as described in section 2.3.1

The presence of amino groups on the sol-gel surface was tested qualitatively by adding Cu (II) stock solution, 1000 mg/L Cu (II), onto the prepared sol-gel. The formation of blue color of copper amine complex was an indication of the amine group.

For amino sol-gel Type 5, the particle size between 100-150μm (100-150 mesh size) were taken and used for further experiments.

2.3.3 Preparation of Ferrozine-Doped Sol-Gel

Type 1: 5 mL TEOS, 5.4 mL ethanol and 1.6 mL de-ionized water were mixed and the mixture was stirred for 30 minutes. 500 μL amino silane was diluted to 1 mL by 1 M HCl and added to the above solution dropwise. The mixture was stirred for 1 hour. Then, 5 mL

100 mg L^{-1} ferrozine solution was added dropwise and the mixture was stirred for additional 1 hour.

Type 2: 4 mL TEOS, 2.0 mL de-ionized water and 0.1 mL 0.1 M HCl were mixed and the mixture was stirred for 30 minutes. 4 mL 10% (w in water) PDMDAAC was added and the mixture was stirred for 30 minutes. 5 mL 100 mg L^{-1} ferrozine solution was added dropwise and the mixture was stirred for additional 1 hour.

Type 3: 4 mL TMOS, 4.8 mL ethanol, 1.92 mL de-ionized water and 100 μL 0.1 M HCl were mixed and the mixture was stirred for 30 minutes. 4 mL 100 mg L^{-1} ferrozine solution was added dropwise and the mixture was stirred for additional 1 hour.

Type 4: 4 mL TMOS, 4.8 mL ethanol, 1.92 mL de-ionized water and 100 μL 0.1 M HCl were mixed and the mixture was stirred for 30 minutes. 4 mL 500 mg L^{-1} ferrozine solution was added dropwise and the mixture was stirred for additional 1 hour.

Type 5: 2.5 mL TMOS, 3 mL methanol and 2.9 mL $0.5.10^{-3}$ M NaOH were mixed and the mixture was stirred for 30 minutes. 3 mL 100 mg L^{-1} ferrozine solution was added dropwise and the mixture was stirred for additional 1 hour.

Then, all sols (Type 1-5) were treated as described in section 2.3.1.

The prepared beads were used as reactive and disposable surfaces and handled by the system equipped with a jet ring cell. The particle size between 100-150 μm was chosen for further experiments.

2.4 Structural Characterization of the Prepared Resins

Scanning Electron Microscope (SEM) images of the prepared resins were obtained in order to have further opinion about the surface morphology. SEM studies were performed using JEOL JSM-6400 Scanning Electron Microscope (SEM). An energy dispersive X-Ray emission spectrometer, EDX coupled to the instrument makes the elemental analysis possible. Differential Thermal Analysis (TA Instr., DMA 983, Dynamic Mechanical Analyzer) were performed to investigate whether there was a structural transition to quartz state.

2.5 Spectrophotometric Studies of Aqueous Solutions of Ferrozine and Fe (II) - Ferrozine Complex

2.5.1 Effect of pH on Iron Complex Formation

The effect of pH on the complex formation of Fe (II) with ferrozine (Fz) was studied in the pH range of 1-11 without using buffer solution. 5 mg L^{-1} Fe (II) and 200 mg L^{-1} ferrozine solutions were prepared in varying concentrations of HCl solutions. The peak signals were obtained by the Shimadzu UV-VIS 160 spectrometer at 562 nm.

2.5.2 Efficiency of Fe (II): Ferrozine Complex Formation in HMTA Buffer

1000 mg L^{-1} ferrozine solution was added to Fe (II) solutions of varying concentrations (0.1-50 mg L^{-1}) prepared in 0.14 M HMTA buffer (Table 2.2) and the complex formation efficiency was studied by the Shimadzu UV-VIS 160 spectrometer at 562 nm.

2.6 Iron Speciation and Preconcentration

2.6.1 Uptake Efficiency of Amino Sol-Gel Resin for Fe (III) and Fe (II)

The uptake efficiency of amino sol-gel resin for Fe (III) cation was obtained by adding 0.1 g resin to 10 ml of pH 4.5 acetate buffer solution (Table 2.2) containing 5 mg L^{-1} Fe (III). The mixture was shaken for 1 hour at room temperature. The resin was removed from each sample by filtration through filter paper (pore diameter: 0.22 μm, Durapore Membrane Filters, Millipore) and filtrates were analyzed for their iron content. The batch capacity was obtained by adding 0.1 g resin to 10 ml of pH 4.5 acetate buffer solution containing 100 mg L^{-1} Fe (III) and the same procedure was applied.

For Fe (II) uptake studies, 0.1 g resin was added to 10 ml of pH 4.5 acetate buffer solution containing 1 mg L^{-1} Fe (II) and the above procedure was applied.

For column type studies, micro-columns (4 cm-length) were prepared from PEEK (polyetheretherketone) tubing (od 3.2 mm, id 2.0 mm). 0.1 g resin (100-150 μm) was packed in the tubing and both ends of the tubing were plugged with small pieces of sponge in order to hold the resin. 10 ml of pH 4.5 acetate buffer solution containing 5 mg L^{-1} Fe (III) was loaded to the column using a Gilson Minipuls 3 peristaltic pump with flow rate of 1.0 mL min^{-1}. The effluent was analyzed for its iron content by AAS.

2.6.2 Recovery and Preconcentration of Fe (III) by Using Amino Sol-Gel

For recovery studies, the resins used for uptake experiments were further exposed to elution cycles performed by 2.5 mL 1 M HCl or 0.1 M EDTA solution, within the filtration system (Advantec MFS, Inc.Glass Microanalysis Filter Holder Assembly).

For column type studies, 2.5 mL HCl was passed through the columns used in uptake experiments. The eluents were analyzed for their iron content.

2.6.3 Uptake Efficiency of Ferrozine-Doped Sol-Gel Resin for Fe (II)

The uptake efficiency of ferrozine- doped sol-gel resin for Fe (II) cation was obtained by adding 0.1 g resin to 10 mL of pH 5.5 HMTA buffer solution (Table 2.2) containing 5 mg L^{-1} Fe (II). The mixture was shaken for 30 minutes at room temperature. The resin was

removed from each sample by filtration through filter paper the effluents were analyzed by both AAS and UV-VIS (Shimadzu UV-VIS 160) spectrometer for their iron content.

The batch capacity of ferrozine- doped sol-gel resin for Fe (II) cation was obtained by adding 0.1 g resin to 10 mL of pH 5.5 HMTA buffer solution containing 50 mg L^{-1} Fe (II). The rest was the same as explained above.

2.6.4 Recovery and Preconcentration of Fe (III) by Using Magnetic Beads (Dynabeads M-270 Amine)

0.050 mL Dynabeads M-270 Amine bead suspension was added to 10 mL of pH 4.5 acetate buffer solution containing 0.050 mg L^{-1} Fe (III).

The mixture was shaken for 1 hour at room temperature. The beads were removed from each sample by magnetic separation with a permanent magnet or by filtration through filter paper. The beads were further exposed to elution cycles performed by 0.1 M EDTA solution, within the filtration system. The eluents were analyzed for their iron content by AAS.

Table 2.2 Compositions of Buffers Used

Buffer	Reagents	Concentrations, M	pH
Acetate	NaOAc	0.1	4.5
	HOAc	0.1	
	$NaNO_3$	0.2	
HMTA	HMTA	0.14	5.5
	HCl	1	

2.7 System Applications

2.7.1 Fe (III) Determination by Using Magnetic Cell

A washing step was necessary to equilibrate the Dynabeads M-270 Amine in the acetate buffer (pH 4.5) solution. The washing procedure is given below:

1. The beads were resuspended by vortexing for 1-2 minutes and the volume to be used was immediately pipetted into a test tube.
2. The tube was placed on a permanent magnet for 4 minutes and the supernatant was carefully pipetted off, leaving the beads undisturbed.
3. The tube was removed from the magnet and the beads were resuspended to the original sample volume in the buffer solution.
4. Steps 2-3 repeated.

50 µL Dynabeads M-270 Amine bead suspension was used for each cycle and perfused by various concentrations of Fe (III) solutions. The preconcentrated Fe (III) was eluted by 0.1 M EDTA solution and transferred on-line to AAS.

The experimental protocol used is summarized below:

1. Bead suspension (Dynabeads M-270 Amine) was aspirated into the holding coil.
2. Sample solution was aspirated into the holding coil and the flow was stopped for a specified contact time.

was stopped for a specified contact time.

3. The flow was reversed through the magnet (magnet on).

4. The retained beads in the flow path were washed with pH 4.5 acetate buffer solution.

6. The eluent (0.1 M EDTA) was aspirated through the flow path and AAS detection started.

7. The magnet was turned off, beads flushed and a new cycle started.

The Fe (III) determination cycle is given in Figure 2.6.

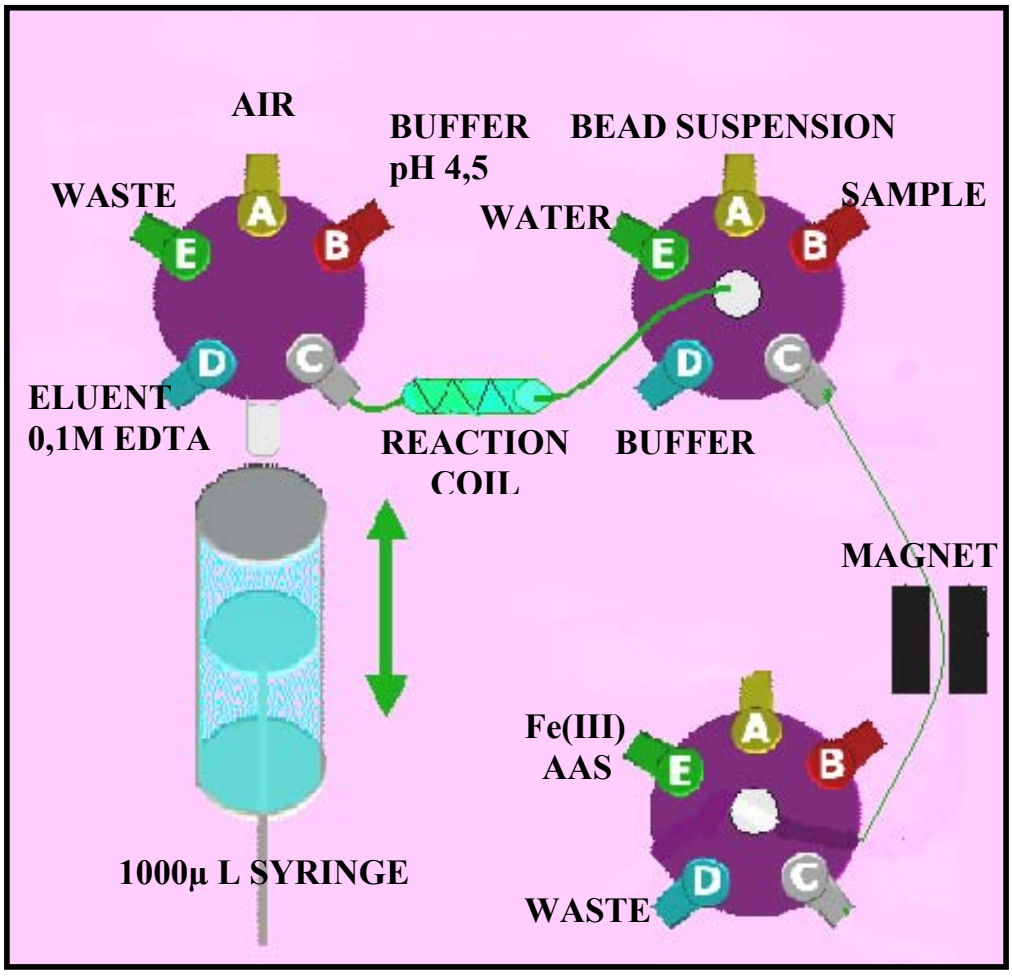

Figure 2.6 Fe (III) Determination Cycle

2.7.2 Fe (II) Determination by Using Jet Ring Cell

Ferrozine-doped sol-gel beads were loaded into the jet ring cell for each cycle and perfused with various concentrations of Fe (II) solutions. The absorbance of the Fe (II)- ferrozine complex was measured on-line at 562 nm with the AvaSpec-2048 UV-VIS FO spectrometer.

The experimental protocol used is summarized below:

1. Ferrozine-doped sol-gel beads were introduced into the jet ring cell.
2. Trapped beads were perfused with pH 5.5 HMTA buffer solution and baseline was established for A or T% measurements.
3. Sample solution was injected and perfused through the beads and the spectrum measurements started.
4. Spent beads were discarded and a new cycle was started.

The Fe (II) determination cycle is given in Figure 2.7.

2.7.3 Optimization of Physical Parameters

The holding coil and reaction coil lengths, flow rates and volumes of reagent and samples used throughout the experiments performed on the FIA system were tried to be optimized.

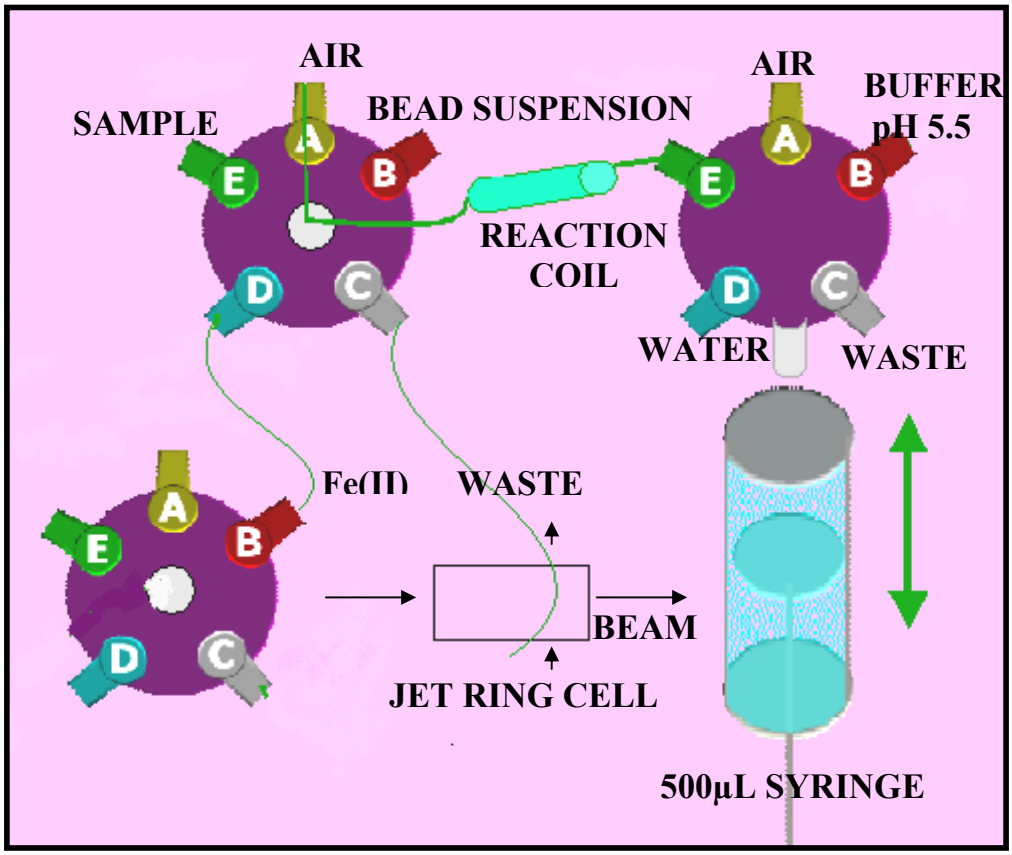

Figure 2.7 Fe (II) Determination Cycle

CHAPTER 3

RESULTS AND DISCUSSION

PART 1

Preparation and Characterization of the Sol-Gel Resins

In this study, two resins were prepared namely; amino sol-gel and ferrozine-doped sol-gel. Their surface characterization studies were performed and the selectivity of the resins to different oxidation states of iron was examined. Batch and column type experiments were carried out to investigate the performance of the prepared resins for the preconcentration and speciation of iron.

3.1 Amino Sol-Gel

3.1.1 Preparation and Characterization of the Sol-Gel Beads

The structure and properties of the sol-gel resins can be modified by varying the synthesis conditions such as the nature and amounts of the silicon precursor, co-solvent and water to alkoxide ratio (R ($n_{H2O}/n_{Si(OR)4}$) and variables such as pH and temperature [2, 4].

At low R values, water is insufficient to complete the hydrolysis process. The measurements indicated that solutions with small water content were comprised of linear polymers when catalyzed by HCl [2].

At low pH, the hydrolysis rate is fast and the condensation rate is relatively low, while higher pH materials have slower hydrolysis rates. Acid catalysts are thought to promote hydrolysis through electrophilic reaction whereas the hydrolysis using base catalyst takes place via a nucleophilic reaction [2].

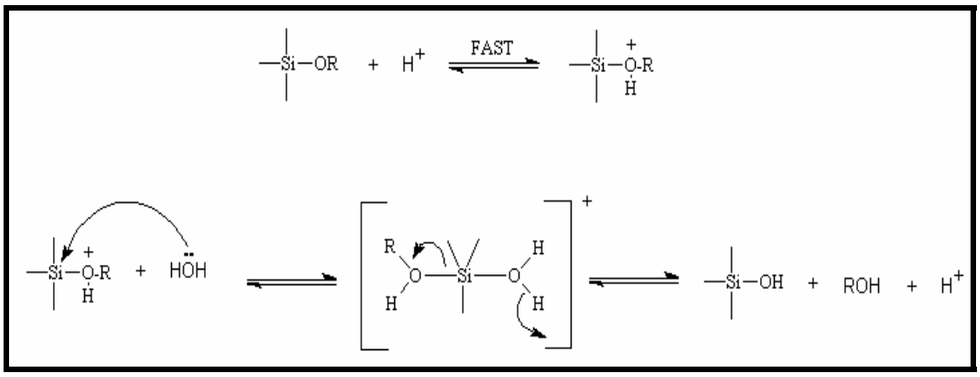

Acid-Catalyzed Hydrolysis

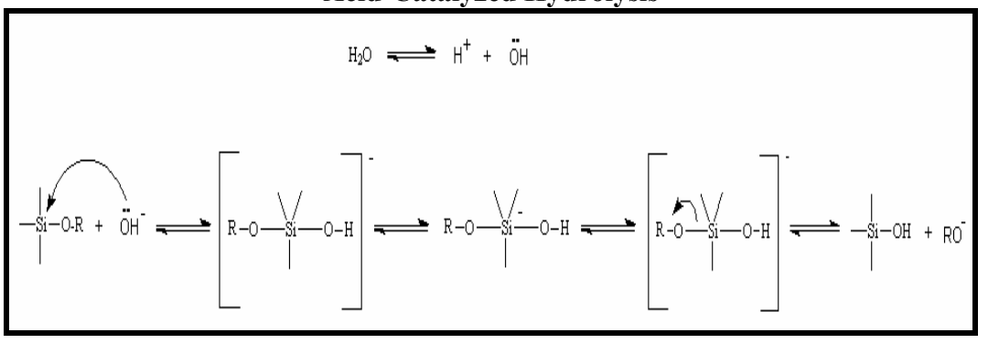

Base-Catalyzed Hydrolysis

Figure 3.1 Acid and Base Catalyzed Hydrolysis Mechanisms

Fast hydrolysis and slow condensation favor formation of linear polymers; on the other hand, slow hydrolysis and fast condensation result in larger, bulkier and more ramified polymers (Figure 3.2). Low pH materials evolve from loose stringy networks, while at high pH, the structure is more colloidal [2].

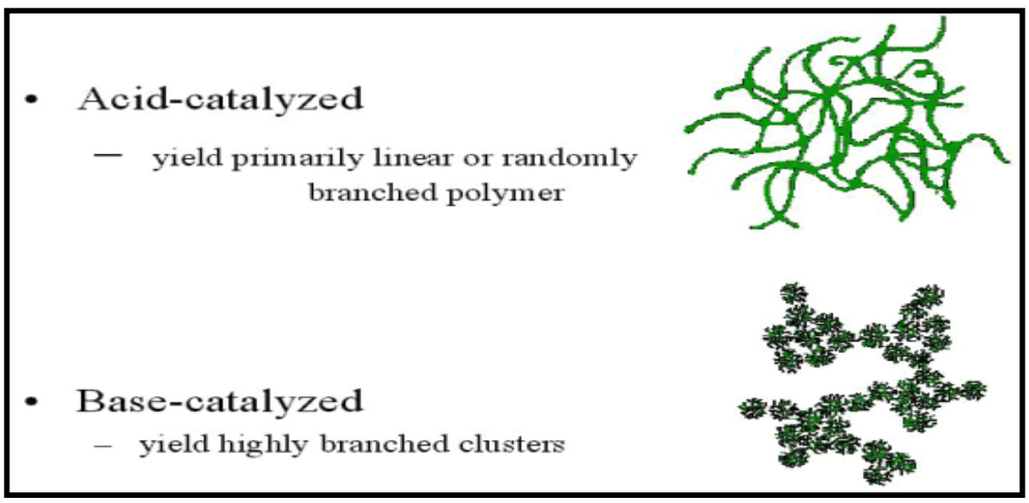

Figure 3.2 Gel Structure for Acid and Base Catalyzed Reactions

In this study, low pH values were used in order to obtain linear and monolithic structures. Due to the compact structure of acid-catalyzed composition, it was considered to be a suitable matrix for the doping and entrapment processes that the entrapped species would be held in the structure effectively without any leaching problem.

The previously used sol-gel compositions which were examined for their Ag(I) capacities [101], were prepared again and their surface characterization studies were performed. The compositions of the sol-gel resins are given in Table 3.1.

Table 3.1 Compositions of the Sol-Gel Resins, ($R(n_{H2O}/n_{Si(OR)4})$

Type	Alkoxide precursor	Acidity	Co-solvent	R
1	TEOS	Acidic	Ethanol	4.0
2	TEOS	Acidic	Ethylene Glycol	25.3
3	TMOS	Acidic	-	2.1
4	TMOS	Basic	Methanol	1.7

The scanning electron microscope (SEM) results (Figure 3.3) indicated that all the sol-gel resin compositions (Type 1-4) have smooth surface and no crystal structure formation was observed.

Sol-gel Type 1 was further dried and densified for X-Ray Diffraction (XRD) and SEM studies. 0.26 g resin (particle size < 75μm) was heated continuously as shown in Table 3.2 and 23.6 % weight loss was observed. The resulting surface was again smooth (Figure 3.4) and the XRD results supported with the differential thermal analysis (DTA) differential thermogram (Figure 3.5) showed no transition to quartz structure (no exothermic peaks). The obtained structure was amorphous.

Table 3.2 Heating Sequence Used for Sol-Gel Type 1

Temperature	Time Interval (min)
100 °C	15
400°C	30
1100°C	180

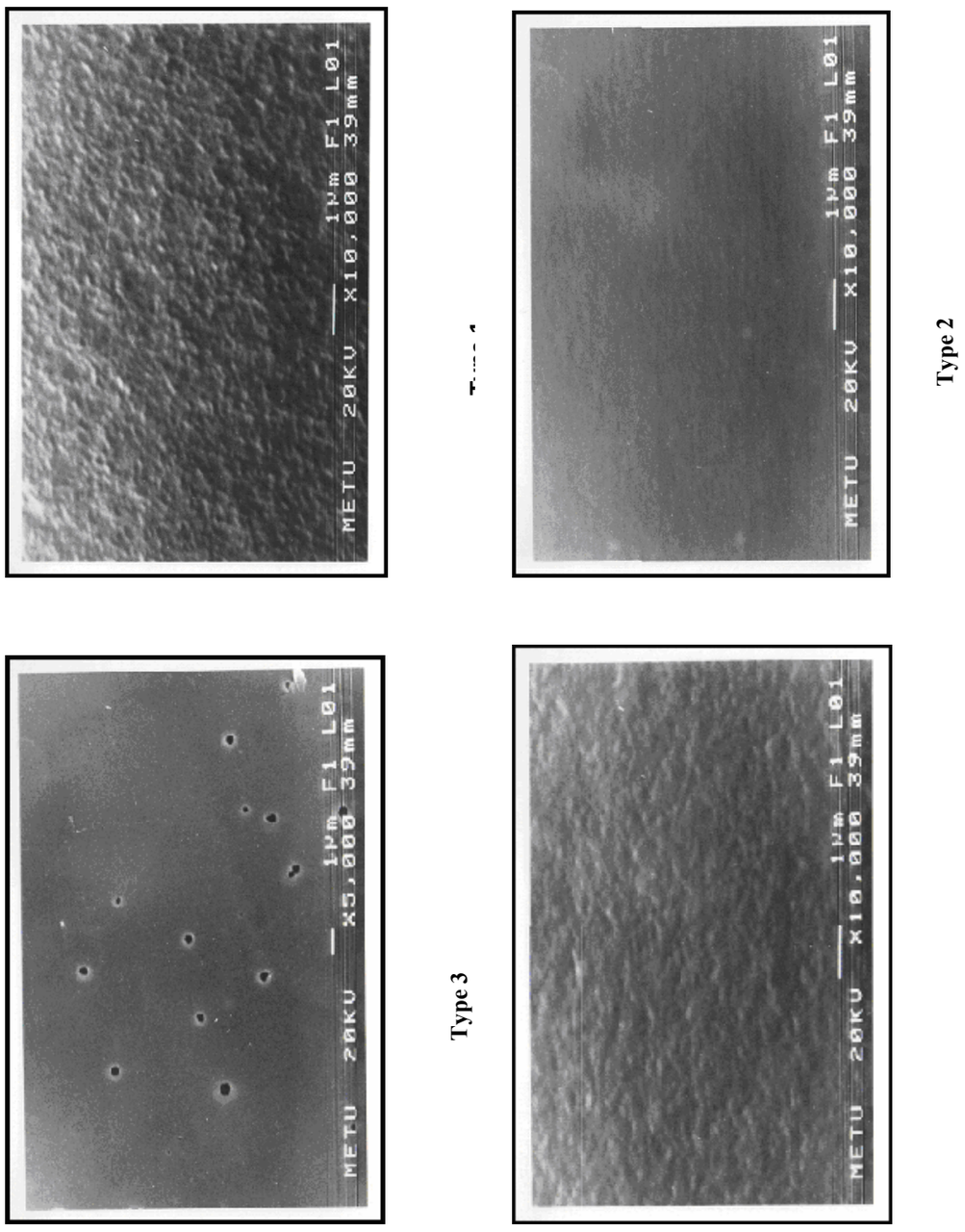

Figure 3.3. Scanning Electron Microscope (SEM) Images of the Sol-Gel Resins

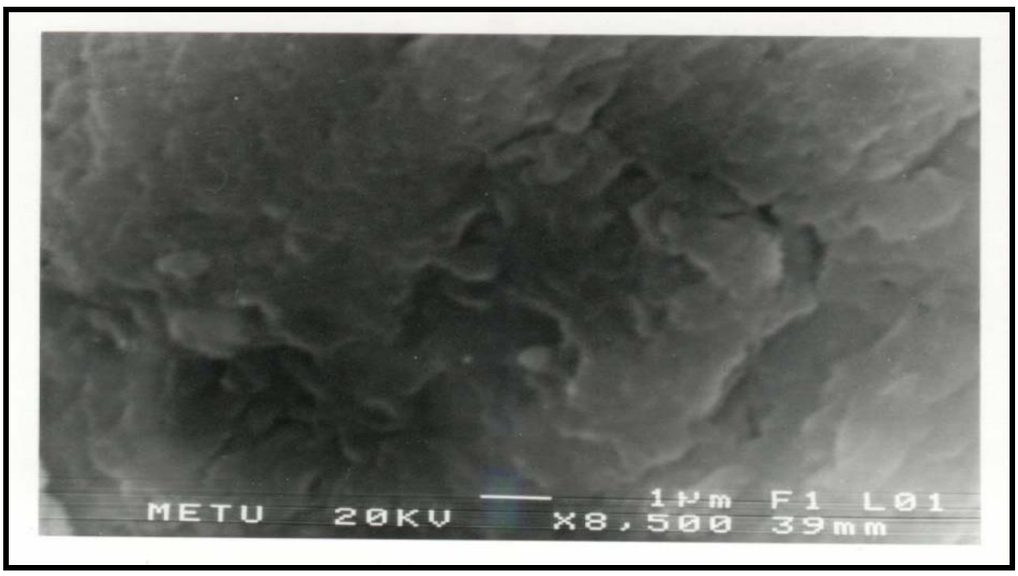

Figure 3.4 SEM Image of Sol-Gel Type 1 (Heated)

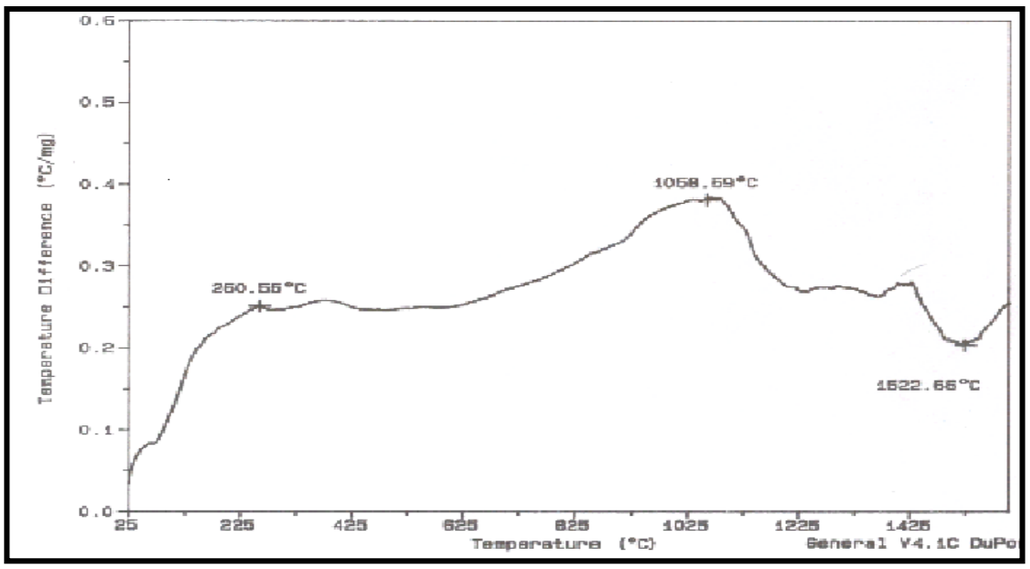

Figure 3.5 Differential Thermogram of Sol-Gel Type 1,
(10 ºC/min, 25-1600 ºC)

3.1.2 Preparation and Characterization of Amino Sol-Gel Resin

Amino sol-gel resin was used for the preconcentration and speciation of iron. It was previously prepared in our laboratory (Table 3.3, Type 1) [101]. The studies performed gave good results for Fe (III) but the structure of the resin was in powder form, which was not suitable for the flow injection system applications. If the solid phase used is in powder form the particle size of the resin could not be controlled (particle size smaller than 75 μm) thus the backpressure in the micro column increases in time and regeneration of the column would not be possible. Therefore, we decided to prepare a monolithic sol-gel structure. By that way, it would be possible to arrange the particle sizes of the resins that can be used for various purposes in the flow injection systems for solid phase extraction studies. The compositions of the amino sol-gel resins prepared are given in Table 3.3.

Table 3.3 Amino Sol-Gel Compositions

Type	Second precursor diluted with	pH	Structure
1	-	11	Powder
2	Ethanol	4.5	Powder
3	Water	3	Powder
4	Ethanol	2	Powder/Monolith
5	1 M HCl	1	Monolith

(Alkoxide precursor: TEOS; second precursor: γ-aminopropyl trimethoxy silane (APTMS); co-solvent: ethanol; R($n_{H2O}/n_{Si(OR)4}$) :4

The addition of APTMS was increasing the pH of the sol unless it was diluted. All the pH values given in Table 3.3 were obtained after the addition of APTMS. As can be seen in Table 3.3, different reagents were used for dilution. The required monolith structure for solid phase extraction studies was obtained in Type 5 composition and used for further studies.

SEM results indicated that the monolith structure (Type 5) has smooth surface (Figure 3.6). DTA studies were performed in order to have more information about the structural characterization of the resin. The exothermic peak between 425 and 625 ºC resulted from the combustion of organic groups. The differential thermogram is shown in Figure 3.7. The structural appearances of the amino sol-gel resins (Type 1-5) are shown in Figure 3.8.

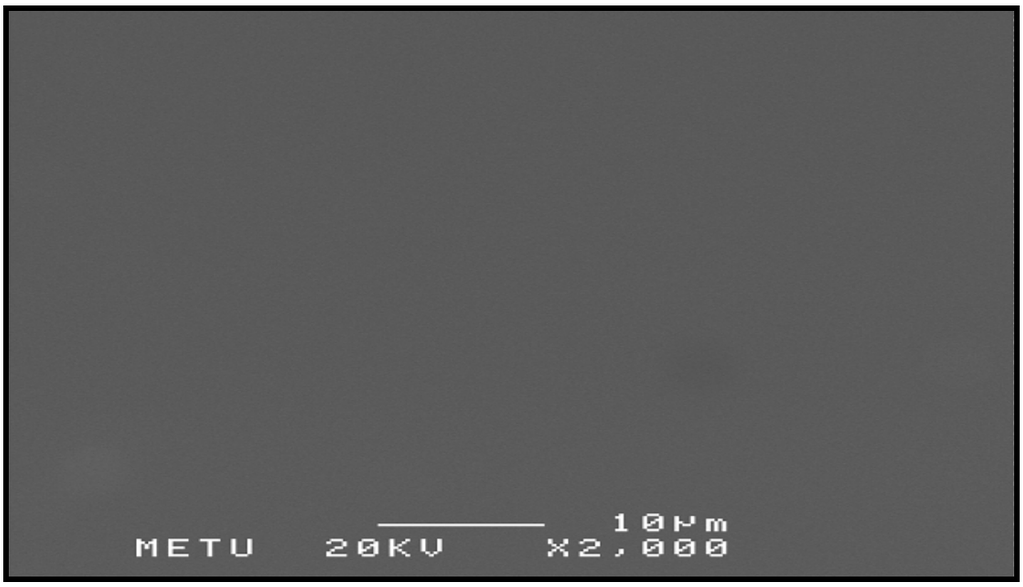

Figure 3.6 SEM Image of Amino Sol- Gel (Type 5)

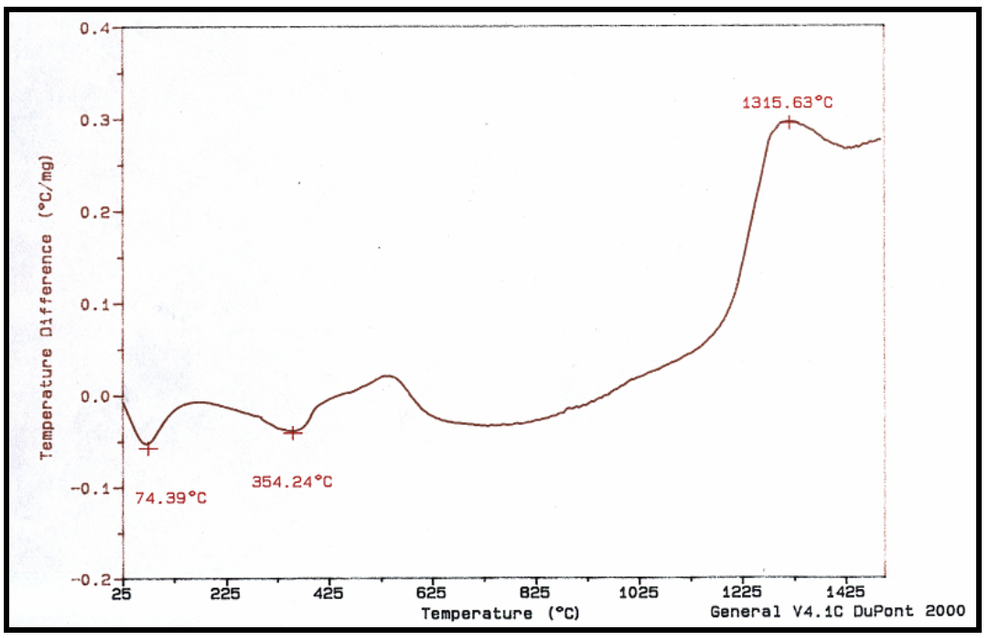

Figure 3.7 Differential Thermogram of Amino Sol-Gel Type 5, (10 ºC/min, 25-1600 ºC)

Figure 3.8 Appearances of the Amino Sol-Gel Resins

3.1.3 Take-up and Recovery Studies of Amino Sol-Gel for Fe (III) and Fe (II)

The optimal pH of iron preconcentration was chosen in regard to both prevention of hydrolytic precipitation of Fe (III) hydroxide and of Fe (II) oxidation to the ferric state. The percent recoveries of Fe (III) and Fe (II) vs pH diagram is given in Figure 3.9.

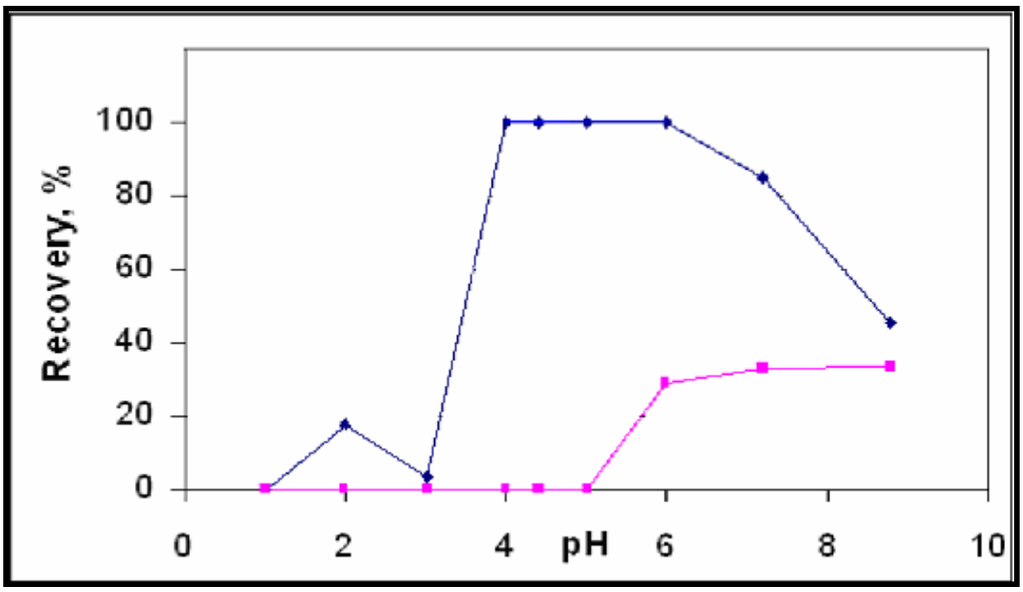

Figure 3.9 Percentage Recovery of Iron Species as a Function of pH (♦ Fe (III), ■ Fe (II)) [101].

Amino sol-gel resin has high affinity for Fe (III) in contrast to that for Fe (II) in the pH range of 4-5. Therefore, pH 4.5 was chosen for further take-up analysis and no interference of Fe (II) was expected [101].

The uptake capacity of the amino sol-gel resin (Type 5) for Fe (III) and Fe (II) was examined and compared with other types of resins.

For this purpose, batch and column type studies were performed. Both types of studies gave the same results so the results were not indicated separately. The types of the resins and % take-up values are given in Table 3.4.

Table 3.4 % Take –up Values of Different Type of Resins for Fe (III) and Fe (II), pH 4.5, n=3

Resin Type	%Take-up for Fe (II), 1 mg L^{-1}	%Take-up for Fe (III), 5 mg L^{-1}	Particle size (µm)	Fe(III) capacity (mmol Fe/ g resin)
Uncoated Sol-Gel	-	62	75-100	-
Amino Sol-Gel (Type 1, powder)	-	100	<75	0.45
Amino Sol-Gel (Type 5, monolith)	5	100	100-150	0.15

For the flow injection studies particle size between 100-150 µm was necessary so the uptake studies for resin Type 5 were performed within this range.

The amino sol-gel Type 1 has higher uptake capacity for Fe (III) when compared to Type 5, which might be due to the particle size differences. As it was mentioned in section 3.2.1, the particle size control for Type 1 was impossible.

The resins used for take-up studies were further exposed to an elution cycle with 1 M HCl and 0.1 M EDTA. The preconcentration factors depend on the starting volume of sample solution and the eluent volume. Elution step by EDTA was slow however with multi-step elution 100% recovery values were obtained. The summary of

preconcentration works and the recovery values for Fe (III) are given in Table 3.5.

Table 3.5 Recovery Analysis of Amino Sol-Gel for Fe (III), pH 4.5, n=3

Resin Type	Sample Volume (mL)	[Fe(III)] (mg L^{-1})	%Recovery (X±%RSD)	Eluent	Concentration factor
Amino Sol- Gel (Type1)	10	5	98±1	1 M HCl	4-fold
Amino Sol-Gel (Type5)	10	5	100±1	1 M HCl	4-fold
Amino Sol-Gel (Type 5)	10	5	77±1	0.1 M EDTA	4-fold

3.2 Ferrozine-Doped Sol-Gel

3.2.1 Preparation and Characterization of Ferrozine-Doped Sol-Gel Resin

The main properties of Ferrozine (Fz) (Figure 3.10) can be stated as follows:

- Forms a 1:3 magenta chelate with Fe (II) which has a sharp absorption peak at 562 nm, (maximum molar absorptivity; 27,000 M^{-1} cm^{-1} at 562 nm)
- Large Fe(II) binding constant (log β_3= 15.6)
- Fe (II): Fz complex stable over a wide pH range (4-9)
- Does not bind Fe (III)

- Melting point: 300 °C (suitable for the sol-gel process)
- Maximum molar absorptivity of Fz; 22,000 M^{-1} cm^{-1} at 283 nm
- Does not absorb visible light [102].

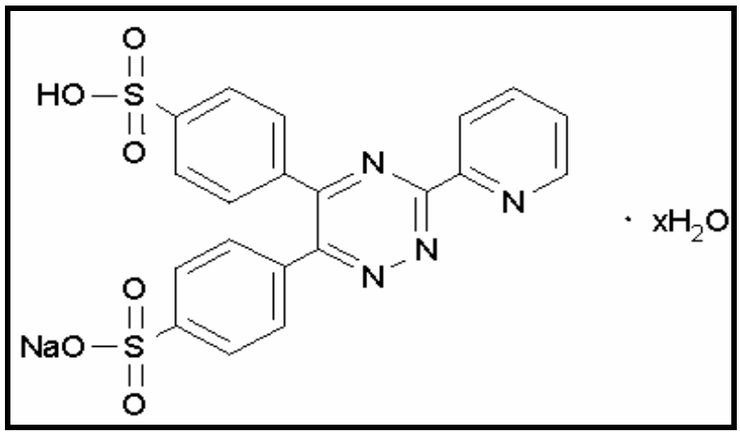

Figure 3.10 Structure of Ferrozine

In order to perform spectrophotometric studies for the determination of Fe (II), Ferrozine-doped sol-gel resin was prepared. Different types of sol-gel matrices were examined for ferrozine entrapment. The compositions of the prepared resins are given in Table 3.6.

The resins prepared were dried to constant weight. The final weight of the resins obtained was between 1.8-2.0 g. This value was used to calculate the ferrozine amount in the resin used.

The stated R ($n_{H2O}/n_{Si(OR)4}$) values indicate the ratio of water and alkoxide used for the sol formation. Aqueous Ferrozine solution was added after the hydrolysis step. The amount of water added in this step was not taken into consideration in the calculation of R values.

The stated R ($n_{H2O}/n_{Si(OR)4}$) values indicate the ratio of water and alkoxide used for the sol formation. Aqueous Ferrozine solution was added after the hydrolysis step. The amount of water added in this step was not taken into consideration in the calculation of R values.

Table 3.6 Ferrozine-Doped Sol-Gel Compositions, R: ($n_{H2O}/n_{Si(OR)4}$)

Type	Alkoxide precursors	Medium	Co-solvent	Amount of Fz doped (µmol)	R
1	TEOS+ APTMS	acidic	ethanol	1	4
2	TEOS	acidic	-	1	6
3	TMOS	acidic	methanol	0.8	4
4	TMOS	acidic	methanol	4	4
5	TMOS	basic	methanol	0.6	10

The SEM results (Figure 3.11) indicated that ferrozine-doped sol-gel Type1, has a rough surface that may be due to the agglomeration of the amino- groups present. The uncoated sol-gel and ferrozine doped sol-gel Type 4 and Type 5 have smooth surfaces and no crystal structure formation was observed.

The DTA results indicated that there was again no transition to quartz state and the resins decomposed above 1400 ºC. The differential thermograms of ferrozine-doped sol-gel Type 4, Type 1 and uncoated sol-gel are shown in Figure 3.12- 3.14.

1. Uncoated Sol-Gel

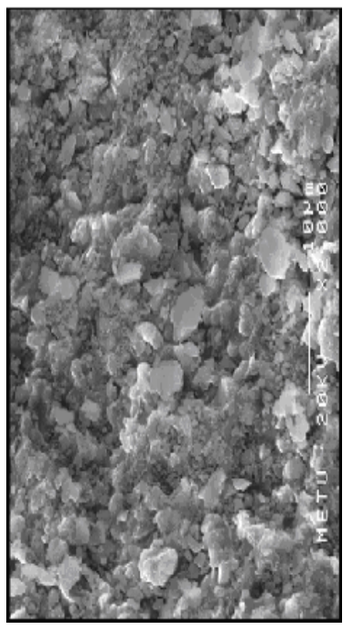

2. Ferrozine Doped Sol-Gel,Type 1

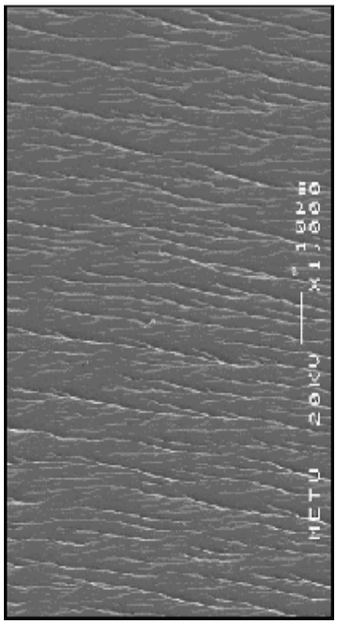

3. Ferrozine Doped Sol-Gel,Type 4

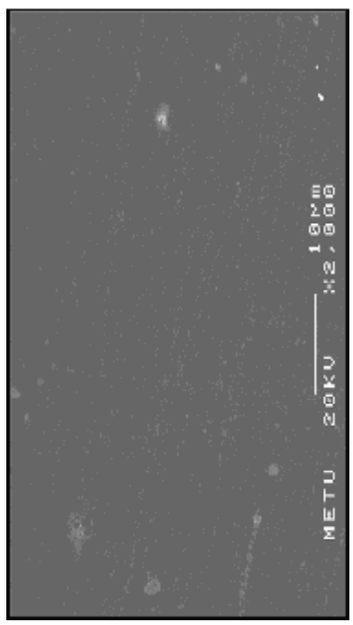

4. Ferrozine Doped Sol-Gel,Type 5

Figure 3.11 SEM Images of Ferrozine-Doped Sol-Gel Resins

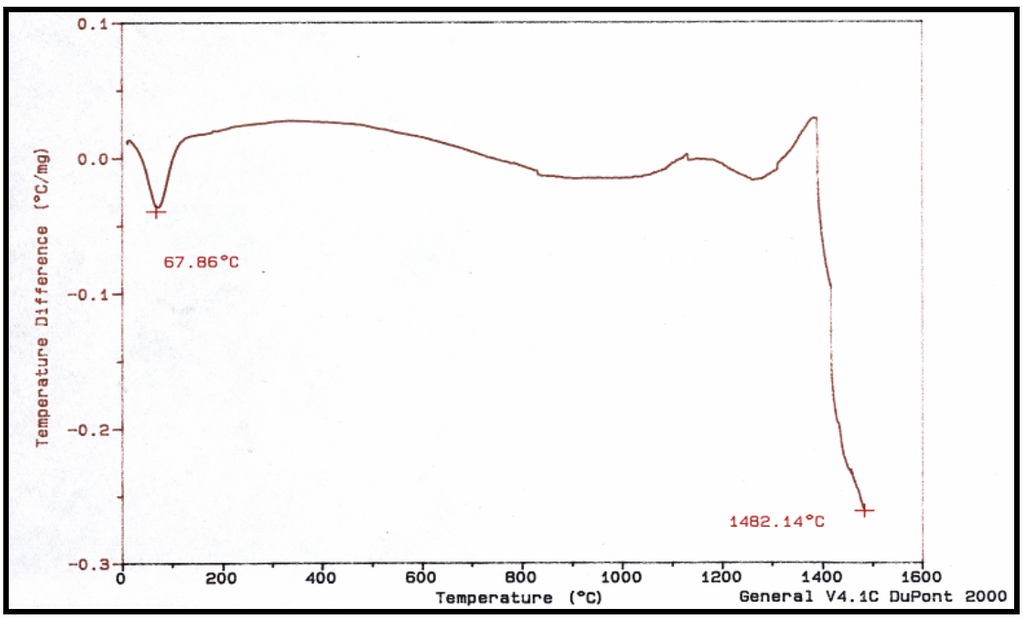

Figure 3.12 Differential Thermogram of Ferrozine-Doped Sol-Gel Type 4, (10 ºC/min, 25-1600 ºC)

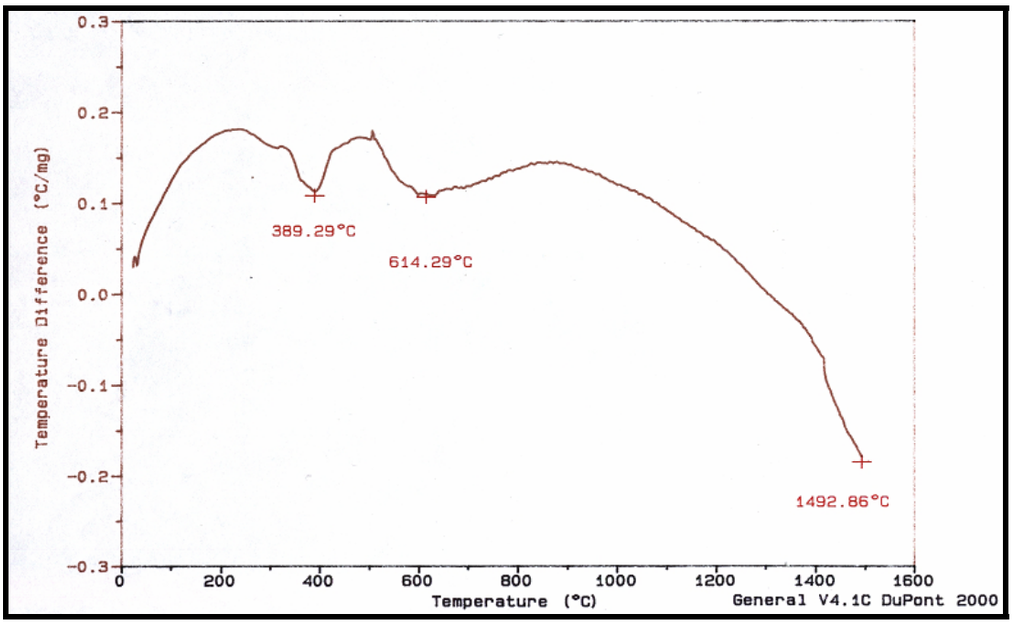

Figure 3.13 Differential Thermogram of Ferrozine-Doped Sol-Gel Type 1, (10ºC/min, 25-1600 ºC)

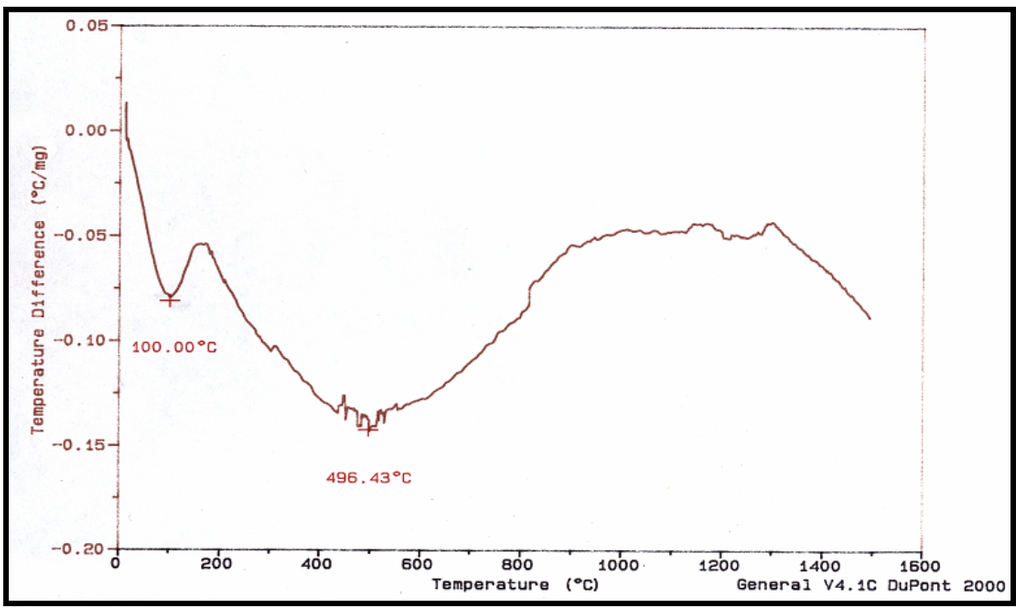

Figure 3.14 Differential Thermogram of Uncoated Sol-Gel, (10 ºC/min, 25-1600 ºC)

The structural appearance of the ferrozine doped sol-gel resins can be seen in Figure 3.15.

Figure 3.15 Appearance of the Ferrozine Doped Sol-Gel Resins

In order to obtain whether the ferrozine-doped sol-gel resin was suitable for spectrophotometric purposes, the UV-VIS spectrum of the uncoated sol-gel **(**containing no Fz**)** composition used in the preparation of ferrozine doped resin was tested for its transparency. The sol-gel monolith used (1-mm thickness) was similar to the one shown in Figure 3.8 (5). A piece of glass was taken as reference and the T% was measured. The result indicated that, the uncoated sol-gel resin has high transparency (Figure 3.16).

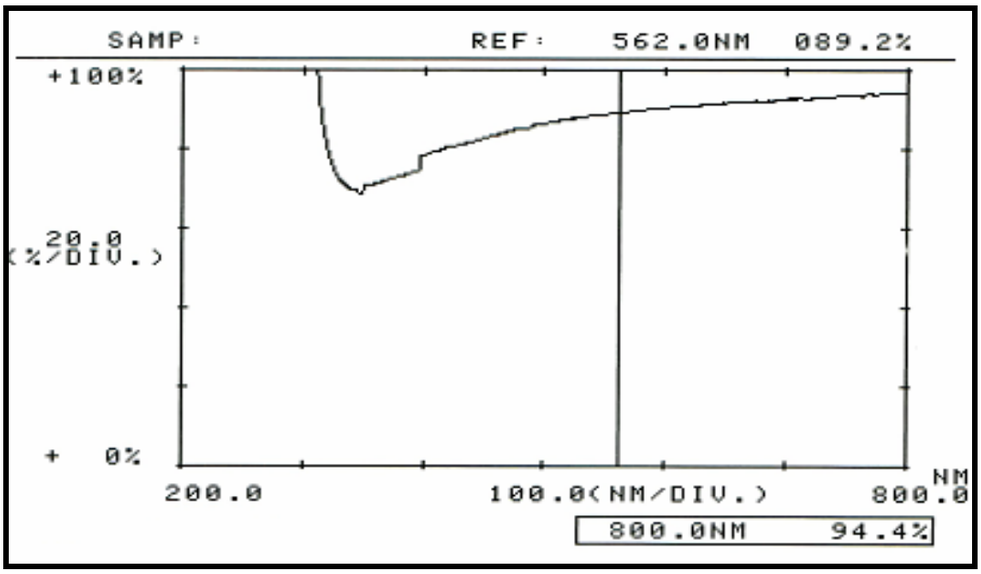

Figure 3.16 UV-VIS Spectrum for Uncoated Sol-Gel

3.2.2 Spectrophotometric Studies of Aqueous Solutions of Ferrozine and Fe (II)-Ferrozine Complex

The wavelength yielding maximum absorbance was identified by first scanning the Fe (II) - ferrozine complex solution over the wavelength range of 200-800 nm with both the AvaSpec-2048 UV-VIS FO (SMA terminated) portable spectrometer and the Shimadzu UV-VIS 160

spectrometer. The maximum absorbance value obtained at 562 nm in both cases was chosen.

Various spectrophotometric studies were performed in order to obtain the suitable pH range for uptake studies, the complex stability and buffer selection. The results indicated that the Fe (II): Fz complex was stable over a wide pH range (4-9) and had maximum peak signals in the pH range of 4-6 (Figure 3.17).

HMTA buffer solution (pH 5.5) which was recommended in the literature [103] was chosen for uptake studies of Fe (II).

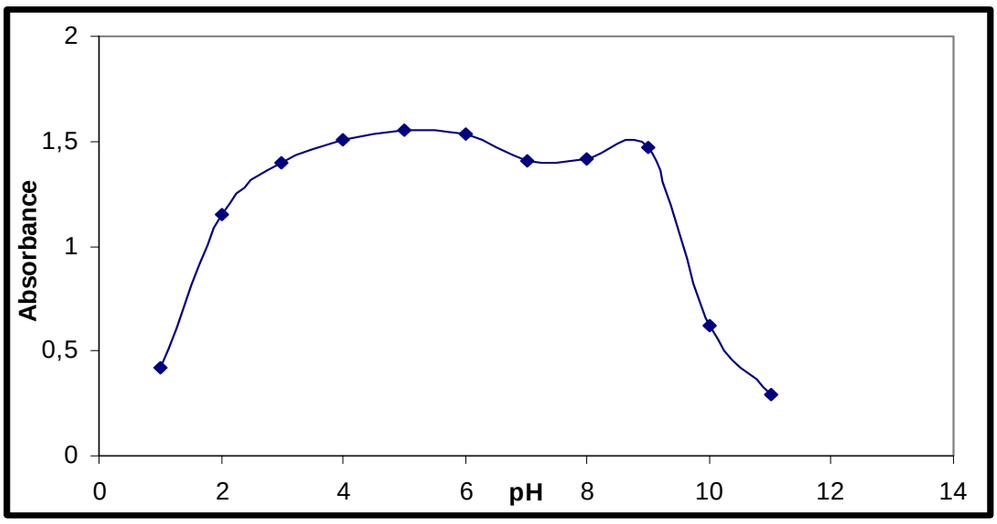

Figure 3.17 Effect of pH on Fe (II): Fz Complex Formation, [Fe (II)] = 5 mg L^{-1}; [Fz] = 200 mg L^{-1}, 562 nm

Calibration curve of ferrozine aqueous solution was plotted by using standard solutions at different concentrations prepared in de-ionized water. The wavelength yielding maximum absorbance was identified by first scanning the ferrozine solution over the wavelength range of

200-800 nm with the Shimadzu UV-VIS 160 spectrometer. The maximum absorbance value obtained at 283 nm was chosen. The linear region is shown in Figure 3.18. This calibration graph was further used to estimate the leached amount of ferrozine from the ferrozine doped sol-gel resin in the solution.

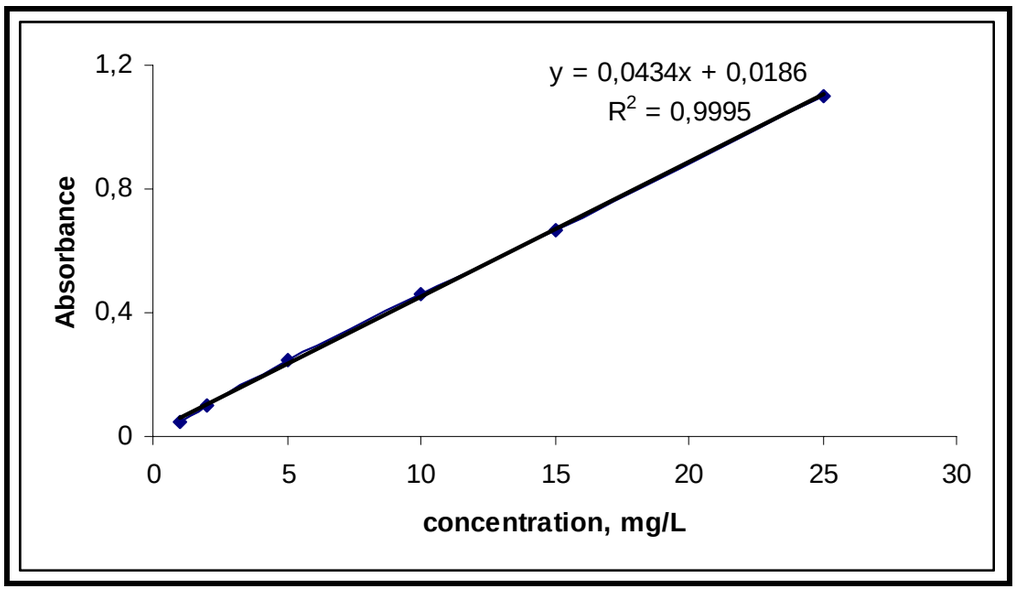

Figure 3.18 Calibration Curve of Ferrozine (λ: 283 nm).

In Figure 3.19 the calibration curve of the Fe (II)- ferrozine complex solution was displayed. Fe (II) standard solutions of various concentrations were prepared in pH 5.5 HMTA buffer and mixed with the same volume of 1000 mg L^{-1} ferrozine solution. As it is seen, the increase in absorbance of the complex was linear up to 10 mg L^{-1} Fe (II) in the presence of 1000 mg L^{-1} ferrozine. The detection limit (3s) was 1.5 ng L^{-1}. This calibration graph was further used to estimate the leached amount of Fe (II) - ferrozine complex from the ferrozine doped sol-gel resin in the solution.

was 1.5 ng L^{-1}. This calibration graph was further used to estimate the leached amount of Fe (II) - ferrozine complex from the ferrozine doped sol-gel resin in the solution.

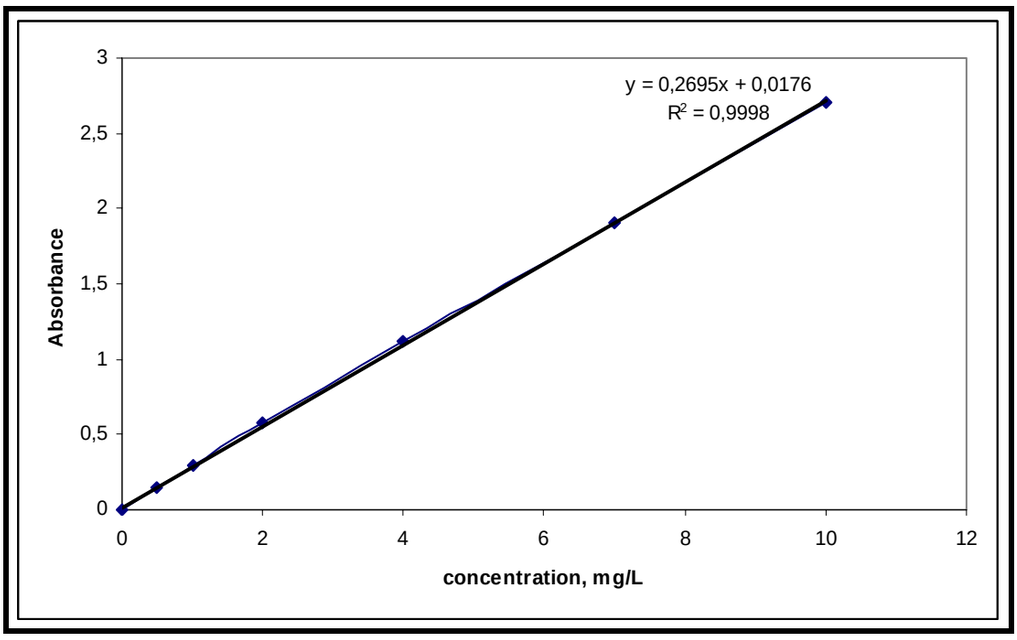

Figure 3.19 Calibration curve of Aqueous Fe (II): Ferrozine Complex Solutions, [Fz] = 1000 mg L^{-1}, λ: 562 nm, pH 5.5.

3.2.3 Take-up Studies of Ferrozine-Doped Sol-Gel for Fe (II)

Only uptake studies were performed for ferrozine-doped sol-gel resins utilizing both atomic absorption and UV-VIS spectrophotometry. Recovery studies were not necessary because the prepared resins were used as recognition surfaces for on-line measurements in the jet ring cell.

i) Atomic Absorption Spectrophotometric Studies

The take-up values for different types of resins for Fe (II) are given in Table 3.7. Capacity measurements were done for resin Type 4, having the highest uptake efficiency.

Table 3.7 % Take-up Values of Ferrozine-Doped Sol-Gel Beads for Fe (II), particle size: 100-150 μm, pH 5.5, n=3

Type	[Fe (II)] (mg L^{-1})	%Take-up	Fe capacity (mmol Fe / g resin)
Uncoated sol-gel	1	29	-
1	5	20	-
2	1	37	-
3	5	95	-
4	5	100	0.054
5	5	23	-

ii) UV-VIS Spectrophotometric Studies

The spectrum of aqueous Fe (II): Fz complex solution was taken (Figure 3.20). As it can be seen, the Fe (II): Fz complex formed gives absorbance peak at 562 nm whereas uncomplexed ferrozine absorbs at 283 nm.

The AAS results showing the highest uptake capacity for resin Type 4 were also supported by UV-VIS measurements. The results proved

that the Fe (II): Fz complex was completely retained on the resin that no signal was observed at 562 nm (Figure 3.21).

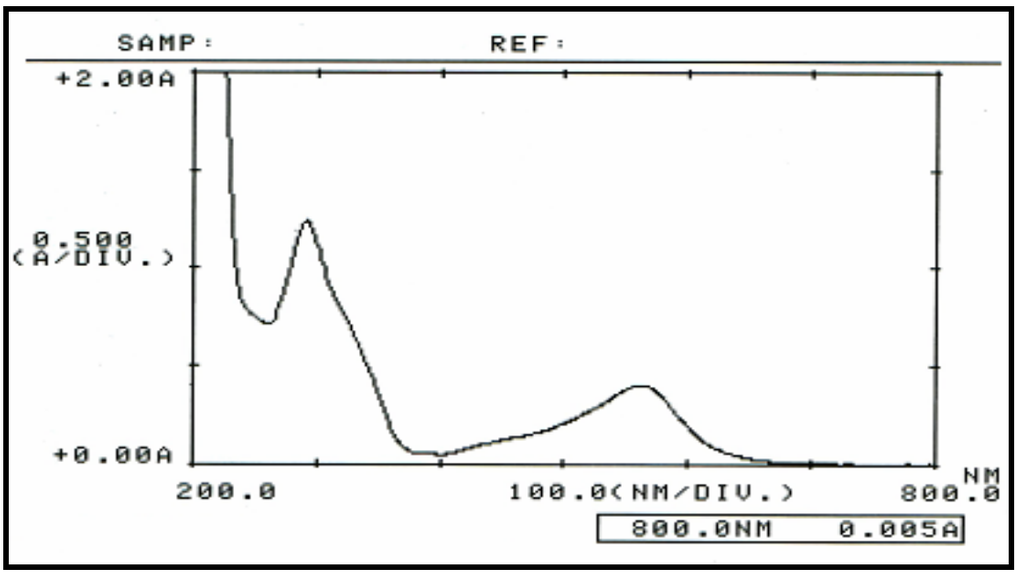

Figure 3.20 Absorbance Spectrum of 2 mg L^{-1} Fe (II) + 100 mg L^{-1} Ferrozine solution, pH 5.5

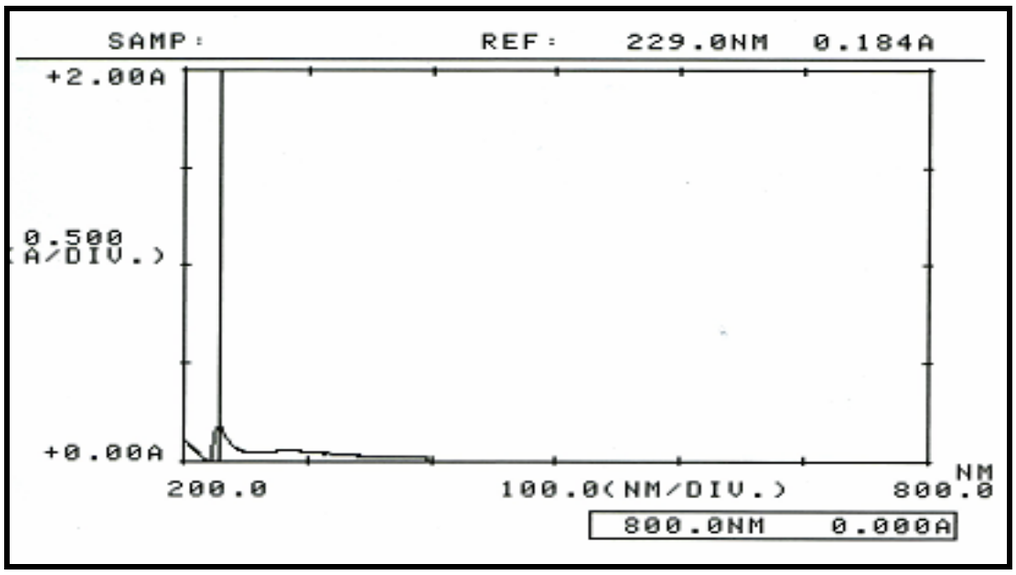

Figure 3.21 Absorbance Spectrum of 5 mg L^{-1} Fe (II) + Fz-doped sol-gel (Type 4), pH 5.5

The uptake efficiency of the ferrozine-doped resin for Fe (III) was also examined. The AAS results indicated that the resin adsorbs Fe (III). However, UV-VIS results showed that there was no interference effect of Fe (III) at 562 nm (Figure 3.22). The signal observed at 283 nm was due to ferrozine leached or the Fe (III) which was not adsorbed on the resin.

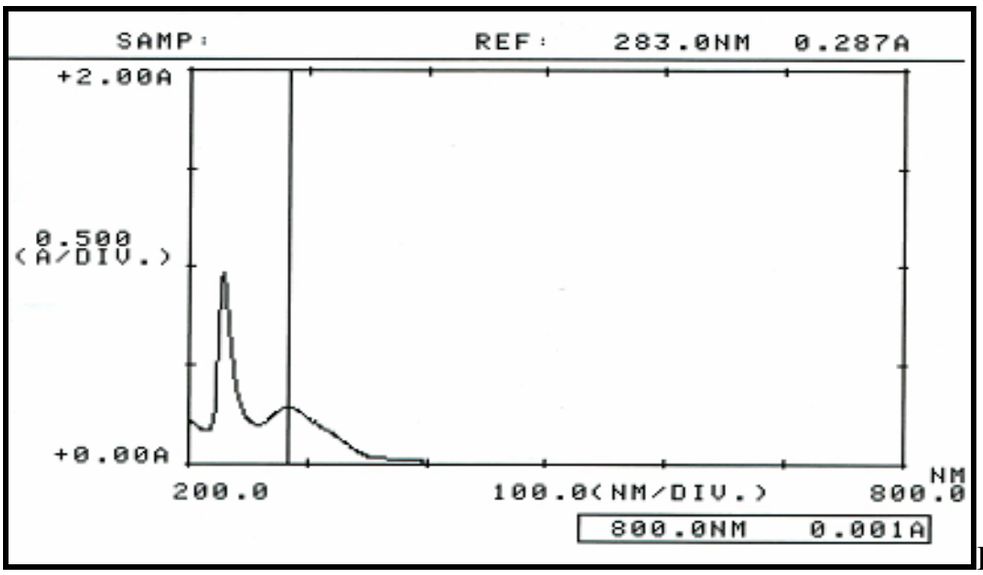

Figure 3.22 Absorbance Spectrum of 5 mg L^{-1} Fe (III) + Fz-doped sol-gel (type 4), pH 5.5

Leaching of the doped reagents hinders their application for water diagnosis. Leaching becomes significant at exceedingly high concentrations of the doped material which may require a pre-washing step for the resin [31]. The ferrozine-doped sol-gel resin was tested for the leaching of the doped material. 0.1 g resin (Type 4) was kept in 5 ml de-ionized water and for 11 days. Then, the resin was removed by filtration through filter paper and the effluent was analyzed for its

ferrozine content. The UV-VIS results indicated that the calculated amount of leached ferrozine (ca. 1 mg L^{-1}) was not noticeable (Figure 3.23).

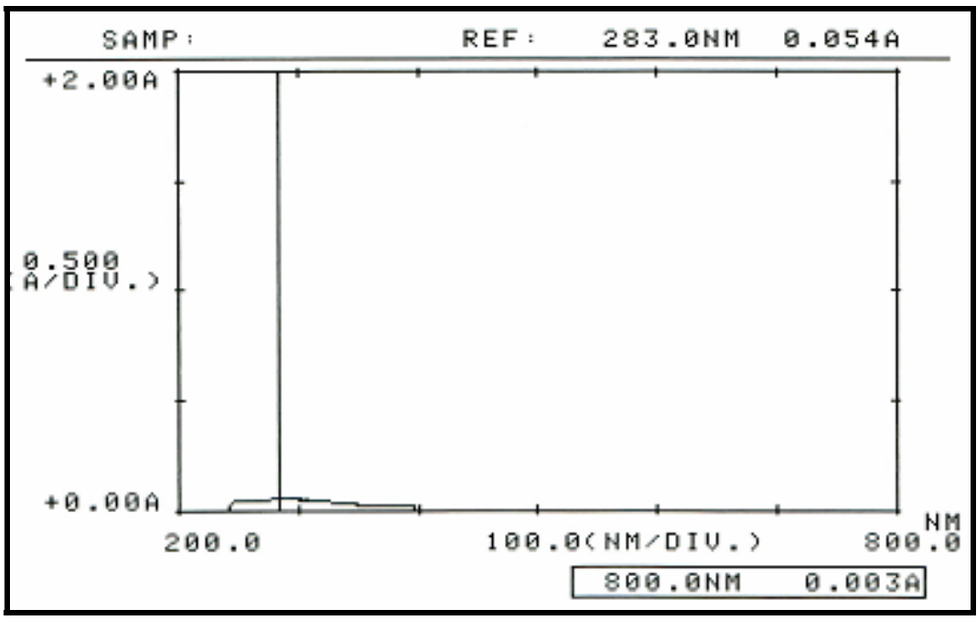

Figure 3.23 Absorbance Spectrum of Leaching Test for Fz-doped Sol-gel (Type 4).

PART 2

Renewable Surface Flow Injection Analysis System (RS-FIA)

In recent years, flow injection (FI) has been used in combination with beads of various solid phase supports. Minute amounts of solid support are reproducibly introduced, handled, captured, perfused, monitored and finally ejected from the flow injection system. Since such a sequence of events will be repeated for each individual measurement, the reactive surface, formed by the particles will be renewed each time [59].

The home-made flow injection system was further modified in order to perform sequential injection and bead injection for the simultaneous determination of Fe (III) and Fe (II) using renewable surface techniques.

As it was indicated, the key component of the RS-FIA system is the flow cell [66-68]. In our studies, a jet ring cell (JRC) and magnetic cell were used as flow cells.

Commercially available magnetic beads coated with primary amino groups and ferrozine-doped sol-gel beads were used as renewable surfaces.

3.3 Fe (III) Determination by Using Magnetic Cell

In order to prepare a versatile renewable surface FIA system a magnetic separation unit was planned to be constructed on our FIA sytem**.** However neither the metal ion studied (iron) nor the resins prepared in this study were suitable for magnetic separation purpose. According to the literature [33- 43], sol-gel matrix is the most convenient host for the preparation of magnetic beads. A joint project with Prof. Dr. Macit Özenbaş (Metallurgical and Materials Engineering Department) was started recently for the preparation of magnetic nano particles using sol gel technology. In order to see the performances of the magnetic separation commercial magnetic beads were used. Since the performance of the amino sol-gel resin for the preconcentration of Fe (III) was investigated extensively in this thesis, the magnetic beads coated with amino groups (Dynabead M-270 Amine) were selected for the on-line preconcentration of Fe (III).

3.3.1 Design of Electromagnets

Two types of electromagnet designs were investigated in this study. These two arrangements have the advantage of viewing the behavior of the beads within the magnetic field. The first electromagnet design began to heat noticeably and was not completely effective in retaining the beads in the flow cell. On the other hand, the second electromagnet design, as shown in Figure 2.4 was successful in the formation of a temporary magnetic bead column. Therefore, this design was used for further experiments.

3.3.2 Design of Flow Cells for Magnetic Separation

Formerly, a spinning Ni wire was placed in the flow channel. Zig-zag bent shaped Ni wires (od 0.2-1 mm) were placed in glass (od 3 mm), Tygon (od 3 mm) and Teflon tubings (od 3.2 mm) of 4.5-9 cm length. The spinning wire serves to sheer the beads off from the wire surface and mix them with the reagent. A Ni wire in a flow tube could act as a magnetic field gradient intensifier so that the beads will pile up on the wire in the flow channel. The use of Ni wire distributes the magnetic field over the entire flow cell and has minimal surface area for carryover. This design had several disadvantages that at some velocity the spinning wire might damage the protective coating on the magnetic particles causing iron contamination and Ni remains significantly magnetic after the first time it is exposed to the magnetic field so that the particles remain stucked on the wire.

As a second approach, the magnetic field effect was aimed to increase by placing the flow cell held in position with a steel sheet. The flow cell consisting of 1.6 mm od Teflon tubing (16 cm length), was wrapped on the steel sheet. The magnetic beads were homogeneously distributed in the flow cell when the electromagnet was on and easily discarded when off. This design was found much more practical and used in further experiments.

3.3.3 The Recovery Studies of Superparamagnetic Beads (Dynabeads M-270 Amine) for Fe (III)

Dynabeads have an even dispersion of magnetic material (γ Fe_2O_3 and Fe_3O_4) throughout the beads. The beads are coated with a thin polymer shell which encases the magnetic material and prevents the leakage of iron in nearly neutral aqueous systems.

The physical characteristics of Dynabeads M-270 Amine (Figure 3.24) are stated as follows

- Diameter: 2.8 μm ± 0.2
- Density: 1.6 g/cm^3
- Magnetic mass susceptibility: 107 ± 19x 10^{-6} m^3/ kg
- Specific surface area: 2-5 m^2/g beads
- Active chemical functionality: 150-175 μmol/ g beads
- Surface charge: positive at pH 2-9
- Iron content: approx. 15%
- Concentration: 2x10^9 beads/ml (approx. 30 mg/ mL) [104].

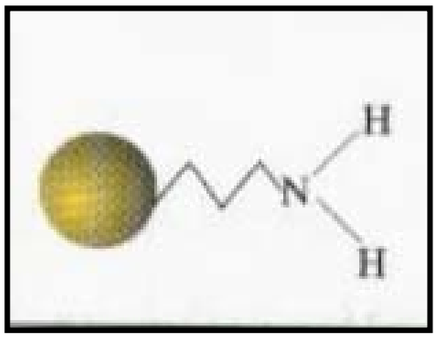

Figure 3.24 Structure of Dynabeads M-270 Amine

As can be seen in the "Take up and Recovery Studies of Amino Sol-Gel for Fe (III) and Fe (II)" part (section 3.1.3), 1.0 M HCl was chosen as the eluent to extract Fe (III) from the amino so-gel resin. However, with magnetic beads it was impossible to use acid for recovery studies that 1 M HCl may possibly leach iron from bead structure and cause contamination during preconcentration studies. Besides, the acid washed beads can not be regenerated. Hence, a new eluent was searched and EDTA was selected for this purpose. 0.1 M EDTA was potent enough to elute Fe (III). The recovery results are given in Table 3.8. The batch type experiments explained in section 2.6.4 gave the same results as given in Table 3.8.

Table 3.8 Recovery Analysis of Magnetic Beads for Fe (III), pH 4.5, n=3

[Fe(III)] ($\mu g\ l^{-1}$)	**Concentration factor**	**Eluent**	%Recovery
50	4-fold	10^{-6} M EDTA	59.6
50	4-fold	0.01 M EDTA	99.2
50	4-fold	0.1 M EDTA	99.4
5	10-fold	0.1 M EDTA	98

The sensitivity of the system which is defined as the concentration of the element that produces an absorbance signal of 0.0044 au was found as 0.050 mg L^{-1}. As can be seen from Table 3.8, the lowest concentration studied on the system was 5 $\mu g\ l^{-1}$ for 10 ml sample solution. By using larger volumes, lower concentrations can be

detected. Although the recovery values were around 99 percent, the iron removal was a slow process compared to that of acid elution**.**
Iron contamination in the case of acid elution of magnetic beads is mainly critical for iron determination. Hopefully for other metals, this problem will not be an important issue.

50 μL of bead suspension was injected for each determination cycle. The optimum flow rate chosen for bead and sample injection was 10 μL/ s.
The holding coil length was 82 cm.

3.4 Fe (II) determination utilizing Jet Ring Cell

Renewable surface technique was also accomplished by combining flow injection analysis with the jet ring cell adapted in this study for measurement of absorbance in UV-VIS spectrophotometry. Ferrozine doped sol-gel resin was used as the recognition surface within the jet ring cell (JRC). The use of jet ring cell is very important because the flow cell must trap the beads in a geometry that allows uniform perfusion and, preferably, simultaneous monitoring of the entire bead layer.

Chemical reactions occur at the bead surfaces and can be analyzed in real time, either directly on the solid phase or within the eluting liquid phase. A multiparameter approach is also possible, by monitoring simultaneously the changes in the solid and liquid phases. At the end of a measurement cycle, the beads can be automatically discarded.

A typical response curve is given in Figure 3.25. The multiwavelength response curve has been obtained by binding nonlabeled opiates antiserum (sheep) on protein G Sepharose 4B beads [59].

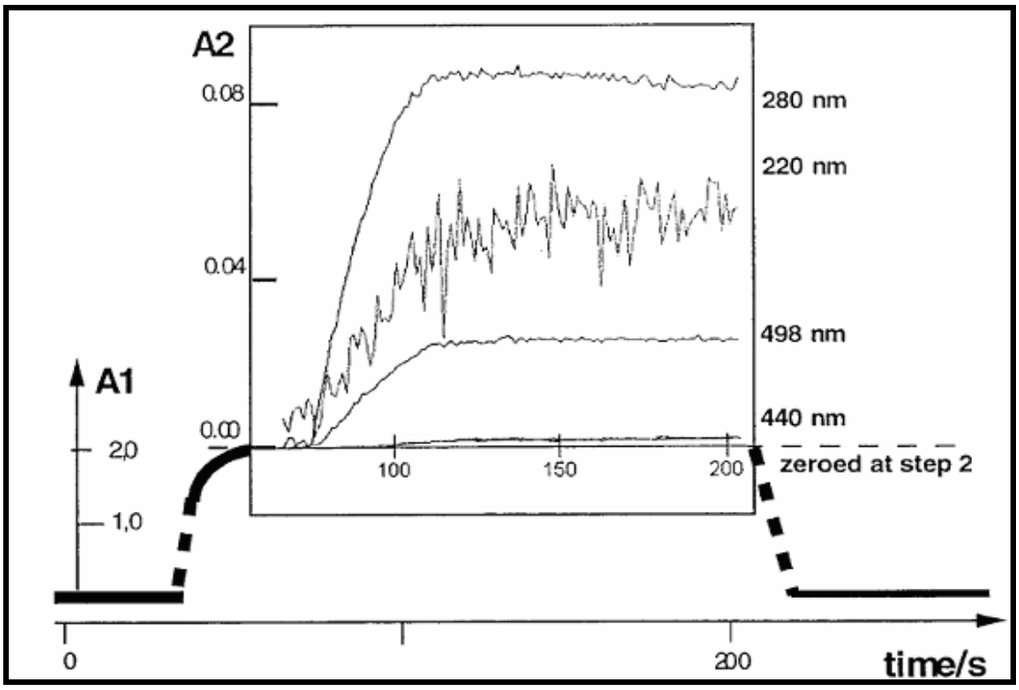

Figure 3.25 Typical Response Curve [59].

The experimental protocol followed in our experiments performed with the JRC was explained is section 2.7.2. 40 µL of ferrozine-doped sol-gel bead suspension was injected into the JRC and the amount of beads trapped in the cell was about 4 µL. Great importance was given not to overfill the cell with beads since the analyte will be first entrapped in uppermost bead layer - outside volume probed by the beam.

All the solutions were aspirated into the JRC from underneath the cell in order to minimize air bubbles. When the jet ring cell was filled with beads the absorbance increasing sharply was zeroed to provide

baseline. Then, the beads were perfused with the solution containing 5 mg L^{-1} Fe (II) and bead surface was monitored continuously. In the last step, beads were discarded (Figure 3.26).

The moving fiber serves as a leaking piston that keeps beads in the flow cell, allowing the liquid to leak around the circumference. When the magnet is activated the stainless steel piston moves to the right, allowing beads to escape [64].

Flow rates during the perfusion step were kept low, typically 2 µL/ s or less. Therefore, 0.5 mL syringe was used as larger syringes cannot generate sufficiently low flow rates. Bead and sample injection was carried at much higher flow rates (50 µL/ s). Baseline was set to zero and data collection started when sample solution started to move out of the injection valve.

The line connecting the valve with jet ring cell and the line between bead container and the valve was kept as short as possible (15 cm).

The volume of bead line was determined. This value was used to program flush volume of bead line and was also added to volume of beads desired to aspirate. In this way bead line was kept free of beads between measurement cycles and when the system was not in use. The position of bead container was slightly off center on the stirring table. This along with bead line inserted all way to container bottom kept beads in suspension, when the table was rotated at about 120 rpm [64].

The response curve of this measurement shown in Figure 3.26 is similar to the typical response curve shown in Figure 3.25.

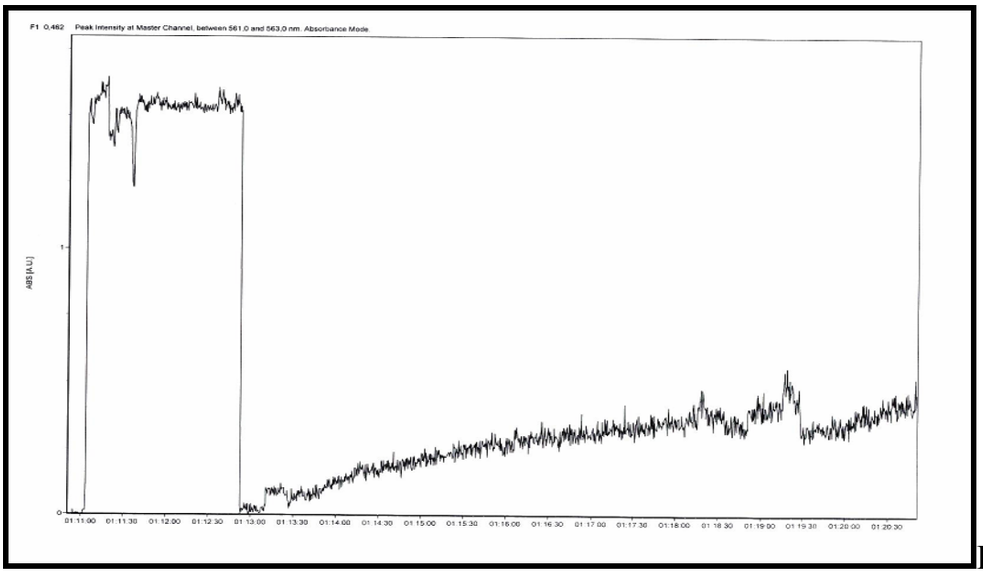

Figure 3.26 Response Curve, λ:561-563 nm,
integration time: 300 ms

The response curves obtained could not be handled because the software that was necessary to convert data to excel (Excel Output) was lacking. A calibration curve could not be obtained and therefore no detection limit and sensitivity was stated for the system. There were also some problems with the fiber optic connections of the jet ring cell. After discarding the beads, the moving fiber connection was not returning to its previous position which might be related to the power supply used. It will be possible to give a detection limit for the system after these problems are eliminated.

3.5 Future Work

The system design will be further modified. The valve positions will be changed and placed close to each other that the length of the connections and relatedly the dead volumes will be reduced drastically. This is especially important phenomena in bead injection analysis (BIA). All the equipments used through and for the flow will be controlled by the flow program (Figure 3.27). Besides the detection limit of the system will be improved. In the future, it is planned to replace commercially magnetic beads with the magnetic sol-gel beads.

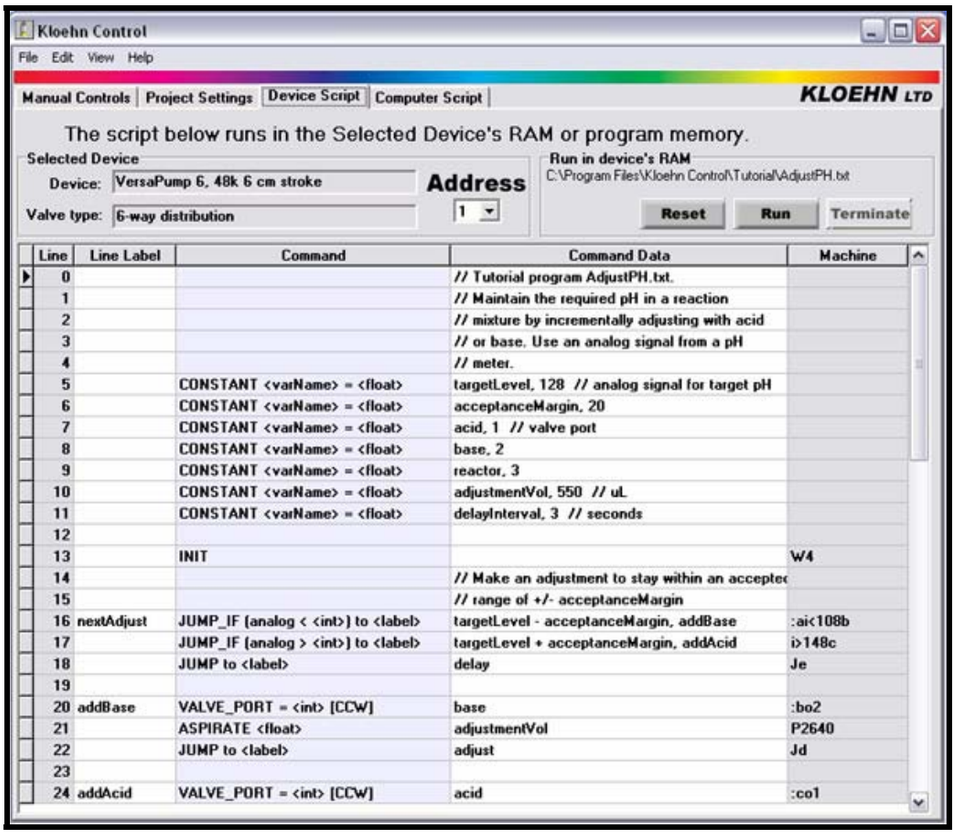

Figure 3. 27 Flow Program

CHAPTER 4

CONCLUSION

The scope of this study was to combine the sol-gel technology and renewable surface flow injection analysis (RS-FIA) techniques for iron speciation and determination.

FIA is a tool for automation of serial assays, together with enhancing selectivity and sensitivity. The reduced sample and reagent handling and reproducibility of FIA have been shown to be useful for improving the time consuming, labor intensive, and traditional separation techniques. In this study a home-made FIA system, which consists of 2 syringe pumps and 3 multi-position selection valves is modified with a jet ring cell and a magnetic cell. The designed system allows the application of all types of flow injection techniques; flow injection, sequential injection and bead injection analysis.

Sol-gel science was used for the preparation of different resins for the preconcentration and speciation of iron. Sol-gel provides a host matrix and many reagents can be doped in the sol-gel structure at the gelation step.

Acidic hydrolysis of tetraethoxysilane (TEOS) or tetramethoxysilane (TMOS) was adapted for the preparation of silica sol-gel resins. Amino sol-gel resin was accomplished by inserting amino silane (γ-aminopropyl trimethoxysilane) as a second precursor. Amino sol-gel has a high affinity for Fe (III) in contrast to that for Fe (II) at pH 4.5.

Nowadays, biologically modified magnetic micro-particles are used in conjunction with the flow injection analysis systems. The use of magnetic beads offers the convenience of magnetic separation. Our aim was to convert the prepared amino sol gel beads into amino superparamagnetic sol-gel beads. A joint project with our Metallurgical and Materials Engineering Department on the preparation of superparamagnetic beads by using sol-gel technology is already initiated. In order to see the performance of magnetic beads in the flow system for the determination of Fe (III), commercial magnetic beads (Dynabeads M-270 Amine), coated with primary amino groups were utilized.

Dynabeads M-270 Amine particles are superparamagnetic, they respond to a magnetic field, but demagnetize completely when the field is removed. Fresh beads are used in each cycle; therefore there is no risk of surface fouling or contamination and no need for a regeneration step of the recognition layer within the system. To the best of our knowledge, this is the first time that magnetic beads are used in the preconcentration of metal ions. The sensitivity of the system for Fe (III) which is defined

as the concentration of the element that produces an absorbance signal of 0.0044 au was found as 0.050 mg L^{-1}.

For the preconcentration of Fe (II), a novel type of sol-gel selective for Fe (II) was prepared by doping ferrozine in the sol-gel structure. The absorbance of the Fe (II) - ferrozine chelate was monitored on-line at 562 nm using jet ring cell connected to the UV-VIS FO spectrophotometer. Batch type analysis for ferrozine-doped sol-gel gave satisfying results. It was also tested on the FIA system but the response curves obtained could not be handled that the software necessary to convert data to excel was lacking. A calibration curve could not be obtained and therefore no detection limit and sensitivity was stated for the system. After these problems are eliminated the system will be used for real sample analysis.

It was considered that the designed RS-FIA system was suitable for the speciation of iron and no interference effect of Fe (II) and Fe (III) on each other was observed.

REFERENCES

1. Mehrotra R.C., “Structure and Bonding 77”, Springer-Verlag Berlin Heidelberg, 1992, 1-31
2. Wright J.D., Sommerdijk N.A.J.M., “Sol-Gel Materials Chemistry and Applications”, Taylor and Francis, London, 2001
3. Uhlmann D.R., Teowee G., Boulton J., Journal of Sol-Gel Science and Technology, 1997, **8**, 1083-1091
4. Brinker C.J., Scherer G.W., “ Sol-Gel Science”, Academic Press Inc., New York, 1990
5. Avnir D., Kaufman V. R., Journal of Non-Crystalline Solids, 1987, **192**, 180
6. Zarzycki J., Journal of Sol-Gel Science and Technology, 1997, **8**, 17-22
7. Pope J.A., Sakka S., Klein L.C., Sol-Gel Science and Technology, American Chemical Society, 1995, 25
8. Collinson M. M., Trends in Analytical Chemistry, 2002, **21**, 30-38
9. De Witte B.M., Commers D., Uytterhoeven J.B., Journal of Non-Crystalline Solids, 1996, **202**, 35-41
10. Vong M.S.W., Bazin N., Sermon P.A., Journal of Sol-Gel Science and Technology, 1997, **8**, 499-505

11. Wei H., Collinson M.M., Analytica Chimica Acta, 1999, **397**, 113-121
12. Maliavski N.I., Dushkin O.V., Tchekounova E.V., Markina J.V., Journal of Sol-Gel Science and Technology, 1997, **8**, 571-575
13. Nivens D.A., Zhang Y., Angel S.M., Analytica Chimica Acta, 1998, **376**, 235-245
14. Chakrabarti K., Kim S.M., OhE.O., Whang C.M., Materials Letters, 2002, **57**, 192-197
15. Kauffmann C., Mandelbaum R.T., Journal of Biotechnology, 1998, **62**, 169-176
16. Reetz M.T., Zonta A., Vijayakrishnan V., Schimossek K., Journal of Molecular Catalysis A: Chemical, 1998, **134**, 251-258
17. Wang R., Narang U., Parasad P.N., Bright F.V., Analytical Chemistry, 1993, **65**, 2671-2675
18. Doelsch E., Masion A., Rose J., Stone W.E.E., Bottero J.Y., BertschP.M., Colloids and Surfaces A: Physicochem. Eng. Aspects, 2003, **217**, 121-128
19. Farias R.F., Airoldi C., Colloids and Surfaces A: Physicochem. Eng. Aspects, 2000, **172**, 145-152
20. Farias R.F., Souza A.G., Nunes L.M., Cardoso V.A., Colloids and Surfaces A: Physicochem. Eng. Aspects, 2002, **211**, 295-298

21. Farias R.F., Airoldi C., Journal of Non-Crystalline Solids, 2000, **26**1, 181-185
22. Farias R.F., Alves S., Belina M.F., Vieira M.R.S., Optical Materials, 2003, **24**, 453-456
23. Hongbing Z., Minquan W., Wenzhe C., Guanghui L., Optical Materials, 2003, **22**, 377-382
24. Zhan H., Chen W., Chen J., Wang M., Materials Letters, 2003, **57**, 1483-1488
25. Zhan H., Chen W., Yu H., Wang M., Materials Letters, 2003, **57**, 1361-1364
26. Sorokin A.B., Buisson P., Pierre A.C., Microporous and Mesoporous Materials, 2001, 46, 87-98
27. Lee J.E., Saavedra S.S., Analytica Chimica Acta, 1994, **285**, 265-269
28. Plaschke M., Czolk R., Ache H.J., Analytica Chimica Acta, 1995, **304**, 107-113
29. Collinson M.M., Critical Reviews inAnalytical Chemistry, 1999, **29**, 289-311
30. Barrero J.M., Camara C., Perez-Conde M.C., Analyst, 1995, **120**, 431-435
31. Kuselman I., Lev O., Talanta, 1993, **40**, 749-756
32. Shi Y., Seliskar C.J., Heineman W.R., Talanta, 1998, **47**, 1071-1076
33. Bruni S., Cariati F., NonoStructured Materials, 1999, **11**, 573-586

34. Solinas S., Piccaluga G., Morales M.P., Acta Materialia, 2001, **49**, 2805-2811
35. Casula M.F., Corrias A., Paschina G., Journal of Non-Crystalline Solids, 2001, **293-295**, 25-31
36. Caizer C., Savii C., Popovici M., Materials Science and Engineering, 2003, **B97**, 129-134
37. Savii C., Popovici M., Solid State Ionics, 2002, **151**, 219-227
38. Zhang H., Wang R., Thin Solid Films, 2003, **429**, 167-173
39. Guo H., Zhao X., Optical Materials, 2003, **22**, 39-44
40. Liu X.Q., Tao S.W., Sensor and Actuators B, 1997, **40**, 161-165
41. Prokes S.M., Carlos W.E., Seals L., Materials Letters, 2002, **54**, 85-88
42. Takahashi R., Sato S., Journal of Catalysis, 2001, **204**, 259-271
43. Ma M., Zhang Y., Yu W., Colloids and Surfaces A: Physicochem. Eng. Aspects, 2003, **212**, 219-226
44. Yan X.P., Hendry M.J., Kerrich R., Analytical Chemistry, 2000, **72**, 1879
45. Obata H., Karatani H., Matsui M., Nakayama E., Marine Chemistry, 1997, **57**, 97
46. Haghighi B., Safavi A., Analytica Chimica Acta, 1997, **354**, 43-50
47. Pullin M.J., Cabaniss S.E., Water Res, 2001, **35**, 363-372
48. Hansen E.H., Analytica Chimica Acta, 1995, **308**, 3-13
49. Ruzicka J., Hansen E.H., Trends in Analytical Chemistry, 1998, **17**, 69-73

50. Ruzicka J., Hansen E.H., Analytica Chimica Acta, 1976, **87**, 353-363
51. Ruzicka J., Hansen E.H., Analytica Chimica Acta, 1980, **114**, 19-44
52. Olsen S., Ruzicka J., Hansen E.H., Analytica Chimica Acta, 1982, **136**, 101-112
53. Ruzicka J., Hansen E.H., Analytica Chimica Acta, 1986, **179**, 1-58
54. Ruzicka J., Hansen E.H., Analytica Chimica Acta, 1988, **214**, 1-27
55. Ruzicka J., Hansen E.H., Analytical Chemistry, 2000, 212-217
56. Ruzicka J., Marshall G.D., Analytica Chimica Acta, 1990, **237**, 329-343
57. Guzman M., Pollema C., Ruzicka J., Christian G.D., Talanta, 1993, **40**, 81-87
58. Holman D.A., Christian G.D., Ruzicka J., Analytical Chemistry, 1997, **69**, 1763-1765
59. Ruzicka J., Ivaska A., Analytical Chemistry, 1997, **69**, 5024
60. Ruzicka J., Scampavia L., Analytical Chemistry, 1999, **4**, 257A
61. Ruzicka J., Gübeli T., Analytical Chemistry, 1991, **63**, 1680-1685
62. Ruzicka J., Christian G.D., Analyst, 1990, **115**, 475-486
63. Cerda V., Cerda A., Cladera A., Trends in Analytical Chemistry, 2001, **20**, 407-418
64. www.flowinjection.com

65. Sole.S, Merkoçi A., Alegret S., Trends in Analytical Chemistry, 2001, **20**, 102-110
66. Chandler D.P., Holman D.A., Trends in Analytical Chemistry, 2000, **19**, 314-320
67. Ruzicka J., Analytica Chimica Acta, 1995, **308**, 14-19
68. Woodbury C.P, Venton D.L., Journal of Chromatography B, 1999, **725**, 113-137
69. Mayer M., Ruzicka J., Analytical Chemistry, 1996, **68**, 3808-3814
70. Ruzicka J., Analyst, 1998, **123**, 1617-1623
71. Sole S., Alegret S., Cespedes F., Fabregas E., Analytical Chemistry, 1998, **70**, 1462-1467
72. Pollema C.H., Ruzicka J., Christian G.D., Analytical Chemistry, 1992, **64**, 1356-1361
73. Bowie A.R., Achterberg E. P., Analytica Chimica Acta, 1998, **361**, 189
74. Christian G.D., Ruzicka J., Analytica Chimica Acta, 1992, **261**, 11-21
75. Ruzicka J., Analytica Chimica Acta, 1992, **261**, 3-10
76. Ruzicka J., Arndal A., Analytica Chimica Acta, 1989, **216**, 243-255
77. Tena M.T., Analytica Chimica Acta, 1997, **343**, 191-197
78. Blain S., Treguer P., Analytica Chimica Acta, 1995, **308**, 425-432
79. Filik H., Öztürk B.D., Doğutan M., Gümüş G., Apak R., Talanta, 1997, **44**, 877-884

80. Lima J.L.F.C., Matos C.D., Vaz M.C.V.F., Food Chemistry, 1998, **62**, 117-121
81. Sakai T., Yanagisawa A., Higuchi K., Teshima N., Ura N., Talanta, 2000, **52**, 153-159
82. Teshima N., Ayukawa K., Kawashima T., Talanta, 1996, **43**, 1755-1760
83. Ye Y.Z., Mao H.Y., Chen Y.H., Talanta, 1998, **45**, 1123-1129
84. Vink S., Boyle E.A., Measures C.I., Yuan J., Deep-Sea Research I, 2000, **47**, 1141-1156
85. Sweileh J.A., Microchemical Journal, 2000, **65**, 87-95
86. Hirata S., Yoshihara H., Aihara M., Talanta, 1999, **49**, 1059-1067
87. Bowie A.R., Achterberg E.P., Fauzi R., Mantoura C., Worfold P.J., Analytica Chimica Acta, 1998, **361**, 189-200
88. Jong J.T.M. , Analytica Chimica Acta, 1998, **377**, 113-124
89. Akatsuka K., Suzuki T., Nobuyama N., Hoshi S., Haraguchi K., Journal of Analytical Atomic Spectrometry, 1998, **13**, 271-275
90. Burguera J.L., Burguera M., Rondon C.E., Analytica Chimica Acta, 1998, **366**, 295-303
91. Yan X.P., Sperling M., Welz B., Analytical Chemistry, 1999, **71**, 4216-4222
92. Fang Z., Ruzicka J., Hansen E.H., Analytica Chimica Acta, 1984, **164**, 23-39
93. Olsen S., Pessenda L.C.R., Ruzicka J., Hansen E.H., Analyst, 1983, **108**, 905-917

94. Bagheri H., Gholami A., Najafi A., Analytica Chimica Acta, 2000, **424**, 233-242
95. Rubi E., Jimenez M.S., Cerda V., Talanta, 1997, **44**, 553-562
96. Kurissery A.T., Satrugnan K., Bhavaniamma V., Talasila P.R., Chonatumatom S.P.I., Analyst, 1999, **124**, 191-195
97. Fang Z., Xu S., Zhang S., Analytica Chimica Acta, 1984, **164**, 41-50
98. Gervasio A.P.G., Luca G.C., Analytica Chimica Acta, 2000, **405**, 213-219
99. Measures C.I., Yuan J., Resing J.A., Marine Chemistry, 1995, **50**, 3-12
100. Imato T., Ohura H., Yamasaki S., Asano Y., Talanta, 2000, **52**, 19-26
101. Eroğlu T., M. Sc. Thesis, "Use of Sol-Gel Beads in Preconcentration", Middle East Technical University, Ankara, 1999
102. www.sigmaaldrich.com
103. Reguera M.I.P., Carmona I.O., Diaz A.M., Talanta, 1997, **44**, 1793-1801
104. www.dynal.no